1966

Preliminary study of the problem of frost deposition upon a cryosurface in forced convection conditions

Gabriel Biguria O.
Lehigh University

PRELIMINARY STUDY OF THE PROBLEM OF FROST DEPOSITION UPON A CRYOSURFACE IN FORCED CONVECTION CONDITIONS

by

Gabriel Biguria O.

A Thesis
Presented to the Graduate Faculty
of Lehigh University
in Candidacy for the Degree of
Master of Science

Lehigh University
Department of Chemical Engineering
Bethlehem, Pennsylvania
1966

CERTIFICATE OF APPROVAL

This thesis is accepted and approved in partial fulfillment of the requirement for the degree of Master of Science.

June 1, 1966
Date

Leonard A. Wenzel
Professor in Charge

Leonard A. Wenzel
Head of the Department

ACKNOWLEDGEMENTS

I thank the Air Products Company for the generous fellowship which supported me and made this investigation possible.

The advice of Dr. L.A. Wenzel is gratefully acknowledged.

The help given by Joseph Hojsak and Steve Polak in the construction of the equipment, was invaluable.

I also thank Joe Maskew who worked one summer in this project as an undergraduate research assistant.

CONTENTS

Figures

Tables

Abstract

The experimental equipment has been constructed to measure the thermal conductivity of frosts which deposit upon a flat plate in the test section of a low velocity wind tunnel. The free stream velocity ranged between 10 ft/sec and 50 ft/sec. The humidity of the free stream varied between 39 grains/lb dry air and 114 grains/lb dry air. Plate temperatures were kept near - 20°F.

Heat transfer coefficients without frost deposition were measured to an accuracy better than $\mp$ 10% maximum error. The most probable error in the experimental Nusselt numbers was $\mp$ 3.4% . Heat fluxes calculated from the Lewis relation and the measured frost surface temperatures, were higher than the experimental heat fluxes. For the lowest humidity run, the calculated heat fluxes were as much as 20% higher than the experimental heat fluxes.

The thermal conductivity and density of frosts which formed near zero degrees Fahrenheit, could be corrolated by the theoretical model of Woodside (41), and fell within the values for the thermal conductivity and density of packed snow.

The assumption made by Libby and Chen (23), that the deposit surface temperature, at the deposit-air stream interface, is constant with time, has been shown to be incorrect.

A theory is proposed which predicts qualitatively, the growth of the deposit and the change of thermal conductivity and density with time.

The frost height distribution along the length of the plate, has been found to be constant after about 1/4 inch from the leading edge of the deposit.

The deposit density has been found to vary as the length to the -1/2 power, for frosts which form under a laminar boundary layer.

At a given frost average temperature, the thermal conductivity of frosts which formed from a low humidity stream, had a higher thermal conductivity than those which formed from a high humidity stream.

A critical height of the deposit has been determined, for the heat fluxes of this investigation, beyond which the boundary layer becomes turbulent.

Introduction

This investigation intends to answer some preliminary questions associated with the problem of frost deposition upon a cryogenic surface in forced convection conditions. It will also describe the experimental apparatus and suggest other investigations which could be carried out with it.

In the initial steps of a study which will corrolate frost thermal conductivity and density at various cryogenic plate temperatures and free stream conditions, and hopefully solve the simultaneous heat and mass transfer problem, the following questions had to be answered:

1. Will the experimental heat fluxes and thermal conductivities be within the expected limits of error?
2. What are the frost thickness and density distributions along the length of a flat plate under the conditions of this investigation?
3. Under a zero pressure gradient, what are the boundary layer characteristics on a flat plate with frost deposition?
4. Is there a difference between the thermal conductivties of frosts which form in a laminar boundary layer, and those which form in a turbulent boundary layer?
5. What is the effect of the gas stream humidity on the thermal conductivity of the deposit?

6. What is the effect of frost surface roughness on the convective heat and mass transfer coefficients?

A literature survey has shown that there is no thermal conductivity and density data, for frosts which form in forced convection conditions between liquid nitrogen temperatures, and zero degrees Farhenheit. However, in the neighborhood of zero degrees Farhenheit, the experimental investigation of the thermal conductivity of low density ice by N.A.C.A. (11), and in the neighborhood of liquid nitrogen temperatures, a study by N.B.S. of frost which deposited on a cylinder in cross flow, will provide some data to compare with the one obtained in this investigation.

This report will review the unsteady state problem and propose some theoretical solutions. Frost structural models will be discussed and a theory will be proposed to explain, qualitatively, the growth of the crystalline deposit.

Presentation of the Problem. Theoretical Considerations.

The deposition of frost upon a cryogenic surface is a commonly encountered phenomena in industrial applications as well as in experimental work. Industry may be interested in the design of a heat exchanger with frost deposition to purify a gas stream, while a researcher in fluid mechanics may be interested in the deposition of frost on cryogenically cooled turbine blades, which will increase the stability of the boundary layer, and improve the performance of the turbine.

To design the heat exchanger, as well as to predict the stability of the boundary layer on the turbine blades, one requires certain physical properties. Since the problem of frost deposition, is one of simultaneous heat and mass transfer, the frost thermal conductivity, the density, and the heat capacity, will , in general, be required to solve this type of problems.

Transient nature of the problem.

The Natural Bureau of Standards, Richards et al (26), conducted an experiment to measure the heat transferred to a liquid nitrogen cooled cylinder. The cylinder was placed, with its longitudinal axis perpendicular to the direction of the air stream, in the test section of a wind tunnel. The air stream velocity, the humidity and the temperature, were carefully controlled. The rate of liquid nitrogen vaporized , due to the heat transfer to the cylinder surface, was measured. From this measurement, the total heat flux to the

cylinder could be calculated. The frost surface temperature was measured with thermocouples brought to the frost surface. The frost thickness was measured by a scale pointer arrangement connected to the thermocouples. These last two measurements were not very accurate, but do show the transient nature of the problem.

If in a given experimental run, the air stream temperature, humidity, and velocity, were kept constant, then, Richards et al (26), observed that the frost thickness increased with time and approached, assymptotically, some constant value. The frost surface temperature increased from the test cylinder surface temperature, to à temperature close to the melting point (32°F). When the frost surface temperature reached 32°F, it was noticed that:

1. The nitrogen boil-off rate approached a constant value.
2. Water formed on the frost surface if its temperature rose above 32°F, and then it diffused towards the inner part of the deposit. The frost surface temperature would then, fall below 32°F , and eventually rise again. This cycle was repeated.

Thus, a condition characterized by an almost constant heat flux and a self regulating frost surface temperature, was approached with time. This condition will be referred to,as the quasi-steady state.

To predict heat and mass transfer rates in the transient

period, requires mass and energy balances around an element of deposited frost. The boundary conditions at the frost-gas interface, are complicated because the net increase in frost thickness, depends not only on the mass transferred from the gas stream, but also, on the amount that diffuses from the frost surface towards the inside of the deposit. The boundary conditions and the analytical studies of Loper (24), and of Libby and Chen (23), require further discussion.

Schematic Representation of Problem

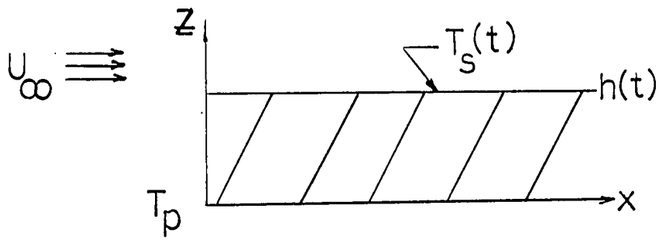

MASS TRANSFER DIAGRAM

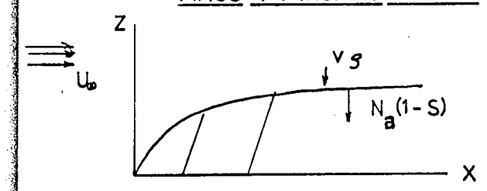

ENERGY TRANSFER DIAGRAM

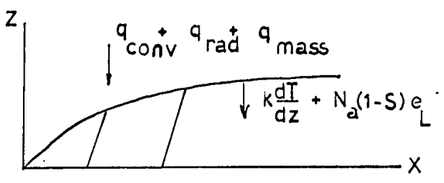

where:

U_∞ = Free stream velocity in the x direction
T^∞ = Static temperature of the free stream
T^∞ = Surface temperature of flat plate
T^p_s = Temperature of frost surface at frost-air interface
h^s = Height of the deposit
v = Velocity component in the normal (z) direction
ρ = Density
e = Specific enthalpy
L = Heat of sublimation of deposit
λ = Heat of vaporization of deposit
N_a = Diffusion mass flux from frost surface to plate surface
k_d = Thermal conductivity of deposit
q^{conv} = Heat transferred by convection to frost surface
q^{rad} = Heat transferred by radiation to frost surface
S = Volume fraction of frost deposit which is solid

The subscripts stand for:

d = property of the deposit
g = property of the gas stream
L = liquid phase

A mass balance at the frost surface gives:

$$-\dot{N}_a\ (1-S) - v_g\ \rho_g = \rho_d\ \frac{dh}{dt} \qquad \text{.....(1)}$$

An energy balance at the frost surface gives:

$$q_{rad} + q_{conv} + (-\ v_g \rho_g\ e_g\ ) = N_a\ e_L\ (1 - S) + \rho_d\ e_d\ \frac{dh}{dt} + k_d\ \frac{dT}{dz} \qquad \text{.....(2)}$$

Substitution of $(v_g\ \rho_g)$ from Eq.(1) into Eq.(2), gives:

$$k_d\ \frac{dT}{dz} + N_a\ (1 - S)\ \lambda = q_{rad} + q_{conv} + \rho_d\ L\ \frac{dh}{dt} \qquad \text{.....(3)}$$

Equation (3) is one of the boundary conditions. The other two are:

$$T(0,t) = T_p \qquad \text{.....(4)}$$

$$T(h,t) = T_s \qquad \text{.....(5)}$$

Libby and Chen (23), made an analytical study of the growth of the deposited layer. They assumed that the conduction within the deposit can be treated as one-dimensional in terms of a coordinate normal to the cold surface. If one assumes that the thermal conductivity of the deposit is a constant, then the following equation describes the transient problem:

$$\frac{\partial T}{\partial t} = \alpha_d \frac{\partial^2 T}{\partial z^2} \qquad \text{.....(6)}$$

where: α_d = Thermal diffusivity of the deposit

Libby and Chen neglected the contributions of the radiation and internal diffusion heat transfer. With this simplifications, the boundary condition represented by Eq.(3) becomes:

$$k_d \frac{dT}{dz} = q_{conv} + \rho_d L \frac{dh}{dt} \qquad \text{.....(7)}$$

Based on an approximate method of Goodman(23), they proceeded to integrate Eq.(7) with respect to z from zero to the moving boundary h, and obtained:

$$\frac{\partial(h\int_0^1 T\, d\eta)}{\partial t} - T_s \frac{dh}{dt} = \alpha_d \left[\frac{q_w}{k_d} - \left.\frac{\partial T}{\partial z}\right|_0 \right] \qquad \text{.....(8)}$$

where: $\eta = z/h$
q_w = Total heat transfer rate
$\left.\frac{\partial T}{\partial z}\right|_0$ = First partial derivative of temperature with respect to z evaluated at $\eta = 0$.

Now, assume a temperature profile across the deposit of the form:

$$T = T_s - (T_s - T_p)(1 - 2\eta + \eta^2) - Q(\eta - \eta^2) \qquad \text{..(9)}$$

where: $Q = q_w h / k_d$

Upon substitution of the assumed temperature profile into Eq.(8), on obtains:

$$2h\left[\frac{dh}{dt}(T_s - T_p) + \frac{Q}{2}\right] + h^2 \frac{dQ}{dt} = -12\alpha_d \left[Q - (T_s - T_p)\right] \qquad \text{.....(10)}$$

Libby and Chen (23) refer to Eq. (10) as " an equa-

tion in two unknowns h and Q " . But Eq.(10) is really an equation with three dependent variables h, Q and T_s, and one independent variable, time (t). The deposit surface temperature (T_s) is a function of time. The deposit height is also a function of time. The variable Q, is a function of T_s and $\frac{dh}{dt}$ as can be seen from the definition:

$$Q = q_w \, h / k_d = \frac{h}{k_d} \left(q_{conv} + \rho_d \, L \, \frac{dh}{dt} \right) \quad \ldots\ldots(11)$$

No attempt was made by Libby and Chen to use the Lewis relation, or any other heat-mass transfer analogy, to make Q a variable only of T_s . Of course, Q also depends on the gas stream velocity and humidity, but both of these variables will be assumed constant for a given deposition problem. If the Lewis relation is assumed to hold, then:

$$h_{conv} = k_y \, c_p \quad \ldots\ldots(12)$$

where:

h_{conv} = Convective heat transfer coefficient
k_y = Convective mass transfer coefficient
c_p = Average heat capacity of gas stream

one can immediately see that Q can be made a variable of T_s only:

$$Q = \frac{h}{k_d} \left(q_{conv} + q_{mass} \right)$$

$$q_{mass} = k_y \, (Y_\infty - Y_s) \, L \quad \ldots\ldots(13)$$

$$q_{mass} = \rho_d \, L \, \frac{dh}{dt} \quad \ldots\ldots(14)$$

where:

Y_∞ = Transferred species concentration in the bulk gas phase

Y_s = Transferred species concentration at the deposit surface.

The development of Libby and Chen will now be continued because of the interesting results obtained at the limiting conditions.

The differentiation of Eq.(10) with respect to time, and the substitution of $\frac{dQ}{dt}$ and Q in Eq.(10), yields a second order equation in h with variable coefficients. To account for the possible effect of mass transfer on heat transfer, the convective heat flux was written in the form:

$$q_{conv} = q_{c,o} + \pi \frac{dh}{dt} \quad \text{.....(15)}$$

where $q_{c,o}$ is the convective heat transfer to the deposit surface without mass transfer, and π is a proportionality factor to account for the possible effect of mass transfer on the convective heat flux. The modified Eq.(10) , can be written in non-dimensional form as:

$$\left[\theta(\pi' + L')\right]H^3\left(\frac{d^2H}{d\tau^2}\right) + \left\{2(\theta-1) + 2\left[1 + \pi'\theta\left(\frac{dH}{d\tau}\right)\right]H + 2L'\theta H\left(\frac{dH}{d\tau}\right) + 12L'\theta + 12\pi'\theta\right\}H\left(\frac{dH}{d\tau}\right) + 12H = 12(\theta - 1) \quad \text{.....(16)}$$

where:

$$H = h\, q_{c,o} / k_d\, T_p$$

$$\tau = t\, q_{c,o}^2 \alpha_d / k_d^2\, T_p^2$$

$$\pi' = (\alpha_d / k_d)\ (\pi / T_s)$$

$$\theta = T_s / T_p$$

$$L' = (\alpha_d\, \rho_d / k_d)(L / T_s)$$

From this point on, Libby and Chen continue to treat θ as a quantity independent of time. However, Richards et al,(26), have found that T_s , and therefore θ , is a function

of time. Nevertheless, Eq.(16) does lead to the following results as τ approaches infinity and as τ approaches zero. When the parameter $\tau \to 0$, the solution will be called the short time solution, and when $\tau \to \infty$, the solution will be called the long time solution.

Short time solution.

One of the initial conditions is that the deposit height is zero at zero time ($H \sim h = 0$ at $t=0$). Libby and Chen assumed the solution for short times to have the form:

$$H = c\,\tau^{1/2} \qquad \text{.....(17)}$$

where c is a constant to be determined. Upon substitution of Eq. (17) into Eq. (16) and the application of the condition $\tau \to 0$, they obtained a long and complicated expression for the value of c. The constant c involves the quantities π', L', and the non-constant variable θ. From physical observations it is evident that as the time approaches zero, the deposit surface temperature approaches the plate temperature, that is, as $\tau \to 0$, $\theta \to 1$. Libby and Chen indicate that their expression for c, is valid for $\tau > 0$ and $c\,\tau^{1/2} \ll (\theta - 1)$, but did not recognize the approach of theta (θ) towards unity as τ approaches zero. If in the limit, as τ approaches zero, one assigns a value of unity to θ in the expression for c, then one obtains:

as $\tau \to 0$, $\theta \to 1$, and $c \to 0$

thus, $c = 0$ in the limit as τ approaches zero.

The result of this discussion is that Eq.(17) does not give values of H from values of γ unless one knows the value of θ at the chosen γ. However, note that since one would not expect θ to be a function of x, if the plate surface is isothermal, and since γ and x are independent, then H, or the height distribution, will be independent of position for short times.

Long time solution.

Libby and Chen have shown from Eq.(16) that H approaches a constant value as γ approaches infinity and the assumptions $dH/d\gamma \to 0$, $d^2H/d\gamma^2 \to 0$. These assumptions are valid even if one considers a non-constant value of θ, because there will be no increase in height after the frost surface temperature has reached the melting point. Thus, the value of the heigth at sufficiently long times is given by:

$$h_\infty = k_d (T_s - T_p)/ q_{c,o} \qquad \text{.....(18)}$$

Note that $q_{c,o}$ is a function of position and varies with x^{-m}, where m = 0.5 for laminar flow. Hence, h_∞ will approach zero at the front edge of the deposit and will increase with x to some power which depends on the flow regime. Note that from its definition γ varies as $q_{c,o}^2$, thus, for a certain value of time greater than zero, γ approaches infinity as $q_{c,o}$ approaches infinity. Since $q_{c,o}$ varies as x^{-m}, then γ will approach infinity near the leading edge. Therefore, the long time solution applies near the leading edge of the deposit.

The solution of Libby and Chen predicts, then, that for some time greater than zero, and (t) time sufficiently long, the deposit will increase from zero at the leading edge, to some value which is independent of x, where the short time solution applies.

Discussion of solution of Libby and Chen.

It has already been mentioned that Libby and Chen made no attempt to use a heat and mass transfer analogy to simplify the boundary condition Eq. (7), and that they did not recognize the fact that T_s, and therefore θ, is a function of time. The heat transferred by radiation to the deposit surface was also neglected in their analysis. The radiative heat transfer at cryogenic temperatures and at the quasi-steady state, is of importance, as can be seen from table I. The mass transfer contribution, for the deposition of water frosts, was calculated from the Lewis relation and laminar flow was assumed. The emissivity of frost was taken from Hsu (19). This value applies to surfaces which have a deposit as small as four thousands of an inch thick.

Table I

Relative contributions to the heat flux

T_s = -200°F	heat flux Btu/hr- ft^2	Percent of heat flux
Radiation	54	4.6
Mass transfer	189	16.0
Convective	924	79.4
Total	1167	100.0
T_s = 31°F		
Radiation	35	10
Mass transfer	127	39
convective	162	51

T_∞ = 80°F , U_∞ = 21.6 ft/sec

R.H. = 50 %

Re = 1.5×10^5

e_{frost} = 0.985

When the surface temperature reaches the melting point, $dH/d\tau$ should equal zero because no more mass is transferred as solid. However, mass will be continued to be transferred as vapor or liquid unless the driving force between the gas stream and the surface is zero. The driving force will be zero when the partial pressure , of the gas which deposits , equals the vapor pressure of the deposit surface.

Let us now return to a discussion of the long time solution. As $\tau \to \infty$, $T_s \to T_{s,min}$, $\theta \to \theta_{min}$, where the subscripts min stand for the condition of minimum heat flux or quasi-steady state. When one considers radiative heat transfer and a non-zero driving force at the quasi-steady state, the heigth of the deposit can be calculated from:

$$h_{oo} = k_d \frac{(T_{s,min} - T_p)}{(q_{conv} + q_{mass} + q_{rad})} \qquad \text{.....(19)}$$

which is very similar to Eq. (18). Equation (19) also predicts that $h_{oo} \to 0$ as one approaches the leading edge.

In the following section a solution is proposed which incorporates a mass transfer analogy to simplify one of the boundary conditions and which does not require a constant value of θ as does the solution of Libby and Chen.

Proposed solution No.1

The Fourier equation for unsteady state heat conduction through a slab (Eq.6) , will be assumed to represent the heat

conduction process through an element of deposited frost.

Other assumptions which will be made are:

1. The heat flux is one dimensional through the deposit
2. The thermal diffusivity is constant
3. The free stream temperature, velocity, humidity , and the plate temperature are constant
4. A heat and mass transfer analogy holds such that the heat transferred at the deposit surface can be calculated if the frost surface temperature is known.
5. The limiting value of the deposit thickness can be calculated from Eq. (19)

The boundary conditions are:

1. $t = 0$, $z = 0$, $q_w = f_1(T_\infty - T_p)$, $T(0,t) = T_p$

2. $t = t_{min}, z = h_{oo}, q_w = f_2(T_\infty - T_{s,min})$, $T(h_\infty, t) = T_{s,min}$

The heat conduction equation is:

$$\frac{\partial T}{\partial t} = \alpha_d \frac{\partial^2 T_2}{\partial z} \qquad \text{.....(6)}$$

If the following dimensionless quantities are introduced:

$$\theta_1 = t / t_{min} \qquad \alpha' = \alpha_d t_{min} / h_\infty^2$$

$$\eta_1 = z / h_{oo}$$

$$T' = (T - T_p) / (T_{min} - T_p)$$

the boundary conditions become:

1. $\theta_1 = 0$, $T' = 0$, $q_w = f_1(T_\infty - T_p)$, $\eta_1 = 0$

2. $\theta_1 = 1$, $\eta_1 = 1$, $T' = 1$, $q_w = f_2(T_\infty - T_{s,min})$

the function f_1 represents the heat transferred to the deposit surface and includes radiation effects.

The non-dimensional equivalent of Eq.(6) is:

$$\frac{\partial T'}{\partial \theta_1} = \left[\frac{d\ t_{min}}{h_\infty^2} \right] \frac{\partial^2 T'_2}{\partial \eta_1} \qquad \text{.....(20)}$$

The solution to Eq.(20) can be obtained by the technique

of separation of variables and has the form:

$$T'(\eta_1,\theta_l) = e^{-\alpha'\theta_l \lambda^2} (A \cos \lambda \eta_1 + B \sin \lambda \eta_1) \quad ...(21)$$

where λ, A, and B, are constants to be determined.

When one applies the condition $\eta_1 = 0$, $T' = 0$, Eq.(21) gives:

$$A \cos 0 + B \sin 0 = 0$$

hence, $A = 0$, and thus:

$$T' = B\ e^{-\alpha \lambda^2 \theta_l} \sin \eta_1 \lambda \quad .....(22)$$

When $\eta_1 = 1$, the heat flux at the deposit surface is f_2:

$$k_d \frac{\partial T}{\partial z} = f_2 \quad .....(24)$$

then, substitution for $\frac{\partial T}{\partial z}$ gives, from Eq(21):

$$(B \lambda \cos \lambda)\ e^{-\lambda^2 \theta_l \alpha'} \left[\frac{(T_{min} - T_p)}{h_\infty} k_d \right] = f_2$$

$$B \lambda\ e^{-\lambda^2 \theta_l \alpha'} \cos \lambda = 1 \quad .....(25)$$

but also, at $\eta_1 = 1$, $T' = 1$, so:

$$T' = B\ e^{-\alpha' \theta_l \lambda^2} \sin \lambda = 1 \quad .....(26)$$

After equating (25) and (26), one obtains:

$$\lambda_m = \tan \lambda_m \quad .....(27)$$

which gives the eigen values of lambda. The first five values of lambda obtained from the solution to Eq.(27) are:

m	lambda(λ)
1	4.58
2	7.75
3	10.9
4	14.06
5	17.22

One can now rewrite Eq.(26):

$$T'(\eta_1,\theta_1) = \sum_{m=0}^{\infty} B_m \; e^{-\alpha' \lambda_m \theta_1} \sin \lambda_m \eta_1 \quad \ldots\ldots\ldots(28)$$

The constant $B_m(\lambda_m)$ is evaluated by multiplying both sides of Eq.(28) by the $\sin \lambda_m \eta_1$, and then by making use of the orthogonality property of the sine function. To evaluate B_m, The following assumption will be made:

A. Assume that when theta (θ_1) equals one, the temperature distribution within the deposit is linear, i.e. a steady state condition exists.

$$T'(\eta_1,1) = \frac{(T - T_p)}{(T_{min} - T_p)} = \frac{f_2 \, h}{k_d} \; (T_{min} - T_p) \quad \ldots(29)$$

$$= \eta_1$$

The final result for B_m is:

$$B_m = \left[\frac{\sin \lambda_m - \lambda_m \cos \lambda_m}{\frac{\lambda_m^2}{2} - \frac{\lambda_m}{4} \sin 2\lambda_m} \right] e^{\alpha' \lambda_m^2} \quad \ldots\ldots\ldots(30)$$

and the temperature equation becomes:

$$T'(\eta_1,\theta_1) = \sum_{m=0}^{\infty} \frac{\sin \lambda_m - \lambda_m \cos \lambda_m}{\frac{\lambda_m^2}{2} - \frac{\lambda_m}{4} \sin 2\lambda_m} \; e^{(1-\theta_1)\alpha' \lambda_m^2} \sin \lambda_m \eta_1$$

$$\ldots\ldots\ldots\ldots\ldots\ldots(31)$$

Equation (31), satisfies the differential Eq.(20), and at least one boundary condition, namely:

$\eta_1 = 0$, $T' = 0$

It is considerably more difficult to show that the second boundary condition is satisfied, that is:

$\eta_1 = 1$, $\theta_1 = 1$, then , $T' = 1$

$$T'(1,1) = \sum_{m=0}^{\infty} \frac{\sin \lambda_m - \lambda_m \cos \lambda_m}{\frac{\lambda_m^2}{2} - \frac{\lambda_m}{4} \sin 2\lambda_m} \sin \lambda_m = 1$$

More work has to be done to show whether or not the second boundary condition is satisfied. On the assumption that (31) is indeed a correct solution, one can obtain by differentiation of (31) and the initial condition:

$$\frac{f_1}{f_2} = \sum_{m=0}^{\infty} B_m \lambda_m e^{\alpha' \lambda_m^2} \qquad \text{.....(32)}$$

Note that from Eq.(32) , one could calculate α' by trial and error or from a graph of Eq.(32) as a function of α'. If one knows α' , then one can calculate t_{min} , the time to reach steady state, which is of practical interest.

The following discussion will deal with the surface conditions of the deposit and it may be very unrealistic because an assumption will be made which has no physical basis. Note that the deposit surface temperature $T'_s = T'(\frac{h}{h_\infty}, \theta)$, is really just a function of height or just a function of time, because it can have only one value at a given height or at a given time.Two methods will be proposed to obtain the relation between the frost surface temperature and time which use the proposed solution No. 1.

B. Assume that the deposit height varies directly as the surface temperature at the frost-air interface.

$$\eta_h = h / h_\infty = T'_s \left(\frac{h}{h_\infty} , \theta \right) \quad .....(33)$$

Equation (33) , satisfies the conditions $T'_s(0,0) = 0$, $T'_s(1,1) = 1$, To arrive at a solution , one would pick a value of η_h , calculate T'_s from Eq.(33), and then by trial and error find the value of theta from Eq.(31).

The idea for the second method of solution was suggested by the assumption of steady state for short times which was made by Loper (24). He assumed that in short time intervals , steady state conditions existed within the deposit such that there was a linear temperature distribution:

$$q_w = f(T_\infty - T_s) = \frac{k_d}{h} (T_s - T_p) = \quad .....(34)$$

thus, if one chooses a value for T_s, h is calculated from Eq.(34) and theta (θ) from Eq. (31) by trial and error.

Proposed solution No.2.

An energy balance around an element of deposited frost which moves with the height , leads to the following equation:

$$k_d \frac{\partial^2 T}{\partial h^2} = \frac{\partial(\rho_d c_p T)}{\partial t} = \frac{\partial(\rho_d c_p T)}{\partial h} \frac{\partial h}{\partial t} \quad ..(35)$$

where the subscripts , except for c_p, represent deposit properties. If the density and heat capacity are independent of height, then:

$$\alpha_d \frac{\partial^2 T}{\partial h^2} = \alpha_d \frac{\partial T}{\partial h} \frac{\partial h}{\partial t} \quad .....(36)$$

A mass balance at the interface, which neglects diffusion,

leads to:

$$\rho_d \frac{dh}{dt} = f_3(T_s) = \text{mass transferred at interface} \quad (37)$$

In this discussion the temperature T will always represent the deposit surface temperature. Substitution of Eq.(37) into Eq.(36) gives:

$$\frac{d^2T}{dh^2} - \frac{c_p}{k_d} f_3(T_s) \frac{dT}{dh} = 0 \quad \ldots\ldots\ldots\ldots\ldots\ldots (40)$$

which is a second order non- linear differential equation. The function f_3 could have the form:

$$f_3 = k_y (P_{oo} - P_s)$$

where k_y is the convective mass transfer coefficient, P_{∞} is the partial pressure in the main stream of the vapor which deposits, and P_s is the vapor pressure of the deposit surface. Equation (40) may be integrated by numerical methods.

Proposed solution No. 3.

This solution is also based on the assumption that the deposit surface temperature varies linearly with the height. A study at Louisiana Polytechnic Institute (6), suggests that this assumption is correct. A mass balance at the frost-air interface, which neglected internal diffusion, lead us to equation (37):

$$\rho_d \frac{d h}{d t} = f_3(T_{oo}, T_s)$$

From the assumption of the linear relation between frost surface temperature and height:

$$T_s = \frac{T_{s,min} - T_p}{h_\infty} h + T_p \quad \text{.....(40a)}$$

When one takes the derivative of Eq.(40a) with respect to time and substitutes for $\frac{d\,h}{d\,t}$ in Eq.(37) one obtains:

$$\left(\frac{h_\infty \rho_d}{T_{s,min} - T_p}\right) \frac{d\,T_s}{d\,t} = f_3\,(T_\infty, T_s) \quad \text{.....(40b)}$$

The above equation can be put in the following form:

$$\left(\frac{h_\infty \bar{\rho}_d}{T_{s,min} - T_p}\right) \int_{T_p}^{T_s} \frac{d\,T_s}{k_y\,(P_\infty - c\,e^{-L/kT_s})} = t \quad \text{..(40c)}$$

which can be integrated graphically or by numerical methods.

P_∞ = partial pressure of condensing gas in main stream
$c\,e^{-L/kT_s}$ = vapor pressure at interface
c = constant of vapor pressure relation
$\bar{\rho}_d$ = average frost density
k_y = mass transfer coefficient

Frost properties.

The equations derived so far have assumed that the thermal properties of frost are known. However, very few investigations have been made to determine frost properties and the scant data which exists is sometimes questionable. The measurement, as well as the prediction of frost properties is complicated by the numerous variables involved. Frost is a porous solid formed by ice and air whose properties are very dependent on the distribution of these two phases.

The frost porosity, which is indicative of the distribution of the ice and air phases, is a function of the environment under which the frost forms. In the case of frost formed upon a cryosurface in a forced convection stream, one would expect the porosity to depend on the temperature of the cryo-surface, the velocity of the main stream, the humidity, and possibly, the degree of turbulence of the air stream, or the boundary layer regime.

To predict the porosity of the deposit, for any given flow condition and plate temperature, is not simple, and more work has to be done in this area. The following paragraphs will try to show the dependence of the thermal conductivity on porosity and frost structure.

The conductivity of a composite material of known composition cannot be predicted by a linear addition of the conductivities of its components (see Ref. 41). A paper which deals with the calculation of the thermal conductivity of porous media by William Woodside (41), reviews the formulas which have been derived for the different structural models. Woodside consired the thermal conductivity of snow near 0 °C and notes that if a a temperature gradient is imposed upon a layer of snow, a corresponding vapor pressure gradient is also set up. The vapor travels towards the cold region in a step fashion. First, some vapor is formed from an ice layer in the warm region. It diffuses

through the air pores, and then condenses on another ice layer. This process transfers the latent heat of evaporation from layer to layer.

Krisher (41) , gives the following expression for the effective thermal conductivity of air in the pores of a material whose pore walls are wetted:

$$k_{eff} = k_{air} + \frac{D}{RT} \frac{P}{(P - P_v)} \frac{dP_v}{dT} \lambda \quad .....(41)$$

$$= \text{cal / cm sec } °C$$

where:

D = diffusion cefficient of water vapor through air cm^2/sec

R = gas constant of the water vapor, g-cm/g

T = absolute temperature, °K

P = air pressure, g/cm^2

λ = latent heat of evaporation, cal/g

P_v = partial pressure of water vapor, g/cm^2

The diffusion coefficient obtained from his experimental results is:

$$D = \frac{239}{P} \left[\frac{T}{273}\right]^{2.3} \quad .....(42)$$

To calculate the snow thermal conductivity, Woodside used the equation:

$$\frac{k_g}{k_{snow}} = 1 - \left(\frac{6\,S}{\pi}\right)^{1/3} \left[1 - \left(\frac{a^2 - 1}{a}\right) \ln \frac{a + 1}{a - 1}\right] \quad .....(43)$$

where: $$a = 1 + \left[\frac{4}{\pi \left(k_s/k_g - 1\right)\left(\frac{6S}{\pi}\right)}\right]^{2/3}$$

$$S = \frac{\rho - \rho_g}{\rho_s - \rho_g} \qquad 0 \leq S \leq 0.5236$$

Subscripts;
s = solid
g = gas

Equation (43) was derived from a model of a porous material in which a unit cube contains one eighth of a solid sphere. The model neglects heat convection effects within the pores. The spheres are assumed not to be in contact and to be distributed in a cubic lattice in a gas. Woodside showed that at 0°C the contribution of the internal diffusion latent heat transfer to the effective thermal conductivity could be as high as 47%.

The model represented by equation(43) is one of many which could be advanced, but actual frost thermal conductivity data is needed to decide which model is closer to reality.

It is apparent therefore, that if one is able to predict the porosity of the deposit for any given flow condition, then one can calculate the thermal conductivity from an equation such as equation(43). No theoretical analysis of this problem could be found in the literature. As a first try in the prediction of the porosity one may hypothesize, based on nucleation theory for solid-vapor nucleation:

1. The mechanism of initial growth formation is through clusters. This will be so if:

$$\Delta H_s < \Delta G_{des} \qquad \text{.....(44)}$$

where: ΔH_s = heat of sublimation of bulk crystals
ΔG_{des} = activational desorption free energy

It is difficult to estimate the desorption free energy. However, from the observed morphology of the frost deposits, one infers thatEq.(44) is satis-

fied and that clusters do form. Cluster formation will not occur when $\Delta H_s > \Delta G_{des}$ (see ref. 16).

2. The volume fraction of solid (S), is proportional to the density of critical clusters, and this density is directly proportional to the rate of impingement of particles upon the substrate.

$$S = c_1 J \quad \text{.....(45)}$$

where: c_1 = some constant which is a function of temperature.
J = mass flux to the surface of the substrate.

3. The rate of change of density of a unit volume sublayer, is equal to the rate of diffusion of vapor from warmer layers.

$$b \frac{d\rho}{dt} = N_a \quad \text{.....(46)}$$

b = height of sublayer within the deposit
N_a = rate of diffusion of vapor

4. The deposit density is a function of J, N_a and time, with the following form:

$$\rho_d = A\, f(N_a, t) + B\, f(J) \quad \text{.....(47)}$$

Note that the impingement flux decreases with time, while the internal diffusion increases with time. From the proposed theory one can predict the following qualitative effects:

1. At the very beginning of deposition, the density will increase until the clusters grow large enough to cross link and form a pattern of growth for the crystals. This process may be very fast.
2. Once a growth patter has been established, the density will tend to decrease because the impingement flux decreases with time, while it will tend to increase because the internal diffusion of vapor increases with time. Since the diffusion does not

become important until the deposit surface temperature is relatively high (see Ref. 38), one can then predict that the impingement flux effect will predominate until the surface temperature reaches a certain value. The density will, therefore, decrease until a minimum is reached, and then , increase continuously with time.

3. Since the thermal conductivity varies with density, one would expect that a qualitative description similar to that of the change of density with time, would apply to the thermal conductivity.
4. The change of the impingement flux with time and the diffusion of vapor to the inside of the deposit, will tend to make the upper layers of frost less dense than those beneath them.
5. The density, and thermal conductivity, will increase with increases in air humidity and velocity because both effects tend to increase the impingement flux.

Barron and Han (2), investigated the deposition of frost upon a vertical plate in free convection at a plate temperature of -310°F and observed that the thermal conductivity passed through a minimum and then increased. This is in accordance with the above theory.

They also observed that the thermal conductivity, up to a mean frost temperature of -260°F, decreased with ambient humidity, see Ref.(2). The discrepancy with the prediction can be explained if one postulates that

until a certain deposit surface temperature is reached, the nucleation occurs in the vapor phase and not upon the substrate. The particles grow before they reach the surface and tend to form a more porous, less dense, deposit. This postulate is supported by their finding that the mass transferred to the substrate was less than that predicted from theory . It is quite possible that the particles which are formed from vapor phase nucleation, retard mass deposition or are simply carried away by the air stream.

In a study at Louisiana Politechnic Institute (Ref.6), it was found that the density increased from the upper to the lower layers as predicted by theory.

The steady state. Information from fluid mechanics.

As has been discussed, the quasi-steady state is characterized by a self controlling condition at the deposit interface which maintains the deposit surface temperature at a nearly constant value. Thus, the problem of heat transferred at the quasi-steady state can be solved if one can predict the boundary layer regime and the roughness of the deposit surface. It is also important to evaluate the effect of the mass flux on the heat and the mass transfer coefficients.

The system which will be discussed consists of a flat plate with a smooth leading edge upon which a stream of air flows in one dimensional , incompressible flow. The main stream is under a zero pressure gradient.

When there is no heat or mass transferred to the plate,

transition from laminar to turbulent flow will occur when a critical Reynolds number has been exceeded. The transition regime , for isothermal flow with relatively low free stream turbulence, extends from a Re of about 1.5×10^5, to a Re of about 3×10^5 (Ref. 28). A stream is considered to have a low turbulence intensity if this value is below 1 % .

When heat is transferred from the stream to the plate, the stability of the boundary layer is increased (Ref. 28), The stability is decreased when heat is transferred from the plate to the stream. The effect of simultaneous heat and mass transfer on the stability of the boundary layer will be investigated.

In a study done in 1961, Kraemer (28) , concluded that a wire which was used to promote early transition was fully effective if:

$$\frac{U_{oo}\ k}{\nu} \geqslant 900 \qquad \text{.....(48)}$$

where:

U_{oo} = free stream velocity
k = roughness height
ν = kinematic viscosity

The value of the constant, 900, will probably increase with simultaneous heat and mass transfer to the plate. From Eq. (48), if the correction for added stability due to heat and mass transfer is known, one can determine if the quasi-steady state will be under a laminar or

a turbulent regime. The value of k in this case would be h_{oo} as calculated from Eq.(19) under the assumption of laminar flow.

To make an estimate of the maximun effect that mass transfer may have on the heat transfer coefficients a mole fraction concentration of $0.05 = x_{\infty}$ will be assumed. Bird, Stewart, and Lightfoot (3), give a detailed analysis of the mass transfer effect. If one uses their Eq. 19.38-28 p.611, to calculate the value of R (21.7-11), one obtains:

$$R = \frac{K \Lambda}{\pi' (0, ,K)} = \frac{x_o - x_{oo}}{1 - x_o} = -0.03$$

The value of x_o, the surface concentration, is very small and will be assumed to be zero. The Schmidt number has a value of about $\Lambda = 0.62$ for air-water vapor systems. With the calculated value of R and the known value of the Sc number, one enters Fig.21.7-1 and obtains $\phi = -0.03$. With this value for ϕ one reads the ratio of the corrected to the non-corrected transfer coefficient from Fig. 21.7-2, and this ratio has a value of 1.02. Thus, a maximum effect of about 2% increase in the transfer coefficients can be expected because of the simultaneous mass transfer.

In the laminar boundary layer, the effect of surface roughness is to advance transition. The critical height is given by Eq.(48) .

In the turbulent boundary layer, if the roughness elements exceed an admissible height given by:

$$k_{adm} \leq 100 \frac{\nu}{U_{oo}} \quad \text{.....(49)}$$

the effect of the roughness elements is to increase the drag and the transfer coefficients from those obtained in a hydraulically smooth plate.

From Eq.(49) one calculates that the admissible roughness, within the turbulent boundary layer, for the conditions of the present investigation, is smaller than nine thousands of an inch high.

Discussion of measurements and equipment.

The measurement of frost thermal conductivity is complicated by the dynamic nature of the process and the numerous variables which affect the conductivity. A continuous or periodic record of eight variables has to be kept.

To measure the conductivity, the assumption is made that the temperature profile across the deposit is linear at any time, although this is only true at the steady state. From an energy balance around the plate one finds:

$$q_w = q_{conv} + q_{mass} + q_{rad} - q_{heat\ leak} = \frac{k_d}{h} (T_s - T_p)$$

.....(50)

where:

q_w = total heat transferred through frost deposit

q_{conv} = heat transferred by convection at frost-air interface

q_{rad} = heat transferred by radiation at fr-air int.ph.

q_{mass} = heat transferred by mass deposited " " "

$q_{heat\ leak}$ = heat transferred to the plate not through frost surface

h = deposit height

T_s = frost-air interface temperature

T_p = plate surface temperature
k_d = thermal conductivity of frost

The average or effective conductivity is calculated from equation(50). Note that q_w, T_s and h, are variables which change with time. To measure q_w the following equation is used:

$$q_w = \dot{m}\, c_p\, (T_{out} - T_{in}) \quad \text{.....(51)}$$

m = mass flow rate of coolant through plate
c_p = heat capacity of coolant
$(T_{out} - T_{in})$ = difference between inlet and outlet temperature of coolant to plate.

In addition to the variables already mentioned, a continuous record of the air velocity, humidity, and temperature, must be kept. The intensity of turbulence of the air stream, the acceleration or deceleration of the main stream, and the boundary layer regime, have to be determined at frequent intervals.

To measure the difference between inlet and outlet temperature of coolant, a sixteen junction thermopile was constructed. Two sixteen-hole , Conax glands were used with No. 30 teflon insulated copper and constantan wires. To test how accurately small temperature differences could be measured with the thermopile, one of the glands was immersed in a constant temperature bath, while the other gland was immersed in an ice bath. The temperature of the bath could be controlled to within $\pm$ 0.01 °F . The temperature of both baths was measured to the nearest thousand of a degree, with an N.B.S. calibrated platinum thermometer. The results of this

test indicated that the thermopile was accurate to ± one hundredth.of a degree for temperature differences between two and five degrees Fahrenheit. The standard thermocouple tables were used to convert the emf. readings to temperature values.

The mass flow rate is measured with a turbine flow meter (Brooks, HP-8N turbine meter, and 4100 frequency converter), The meter is equipped for low temperature measurement of flow . Its capacity is from 0.5 to 5 gpm. The output d.c. signal from the meter frequency converter is recorded continuously. The turbine flow meter was calibrated by Brooks, and is accurate to ± 0.25 % of full scale flow.

The plate surface temperature is measure by taking the average reading of three thermocouples located on the underside of the plate. Calculations showed that a maximun error of 0.5 °F could arise because the thermocouples were not located on the top surface of the plate. The three constantan - copper thermocouples, were calibrated with the same N.B.S. calibrated platinum thermometer and constant temperature bath which was used for the thermopile test.

A Leeds and Northrup, type 31-3, rotary selector switch is used with the three calibrated thermocouples discussed above. The switch is designed to minimize the emf which could be introduced by metals which are different from those used in the thermocouples.

The measurement of the frost surface temperature, at

the frost-air interface, is particularly difficult because anything which touches the frost surface will disrupt the deposit and might trip the boundary layer. A Barnes Eng. Co., optical radiometer was purchased which enables one to measure the surface temperature of any object at a distance. The radiometer-thermometer, has a range from -50°F to + 150°F. For objects whose emmisivity is close to one, the absolute accuracy of the temperature readings is $\pm$ 2°F above 32°F, and $\pm$ 4°F at the lower range of the temperature scale. However, the reproducibility of the measurements is within less than a degree, at least in a period of about four hours, so that by calibrating the scale at the ice point , and at room temperature, before each run, one may obtain an accuracy of $\pm$ 1°F or better. Note that according to Hsu (19) , frost has an emmisivity of 0.985 for deposits as small as four thousands of an inch thick.

The air stream temperature is measured with a three junction thermopile. The air stream wet bulb temperature is measured with a three junction thermopile fitted with a wick which keeps the thermopile saturated with water. Both thermopiles were calibrated against an N.B.S. calibrated (test N. 127170) mercury thermometer. The output of the thermopiles is read from a recorder to the nearest tenth of a degree. Temperature readings can be corrected to account for the dynamic heating of the thermopiles.

The correction at 50 ft/sec, the highest speed attainable in the wind tunnel, corresponds to about 0.5°F.

One of the most difficult variables to measure is the frost height. An apparatus was designed which is able to measure the thickness of the deposit by optical means and is sensitive to a change in thickness of 0.0001 inch. The accuracy may vary according to the maximum height to be measured, but for most measurements in this study, the accuracy is about $\mp$ 0.003 inches. The output from the instrument is recorded continuously and the response is practically instantaneous.

The optical profilometer discussed above, consists of a photomultiplier (pmt),tube, two slits, one convex lens, and a constant light source. A photomultiplier tube reacts to the light which impinges upon its active surface . A cascade of electrons multiplies the effect of the phonons which strike the active surface and makes the tube ex - tremely sensitive to the light which strikes it. A great variety of tubes is available and the region of the light spectrum at which they are most sensitive, varies considerably. The output of the photomultiplier tube is directly proportional to the intensity of light which strikes it.

The instrument works in the following manner:

A well collimated beam of light strikes the photomultiplier tube. The beam of light is obstructed only by the frost as it builds up over the test plate. Since the output of

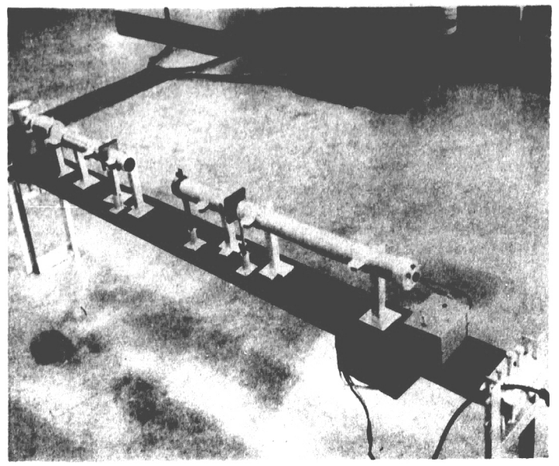

Fig. 1 : Optical Profilometer

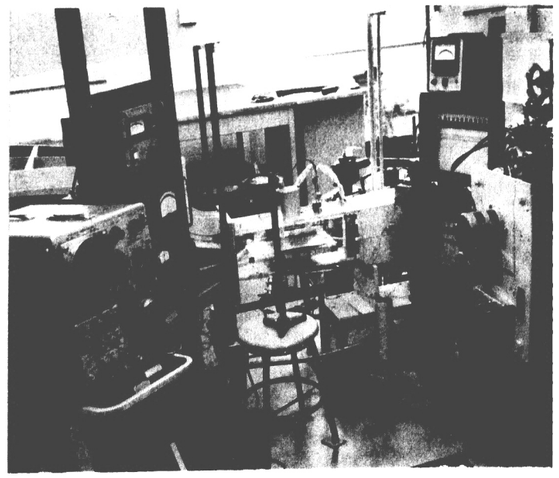

Fig. 3: Instruments on West Side

the photomultiplier tube is directly proportional to the intensity of light incident upon it, within the linear range of the tube, and since the intensity of light which strikes the tube is directly proportional to the area through which the beam of light can pass, the output of the photomultiplier tube is, thus, inversely proportional to the height of the deposit.

Tests to prove the preceeding argument were made during the summer of 1965, and even with a crude set up, a linear response accurate to within $\mp$ 0.005 in. was obtained. There were problems with noise introduced by stray A.C. current, but the use of well insulated wire solve this problem. Noise in the output also was found to come from the light source which initially was a mercury lamp. Instead of the arc lamp, a 6 volt bulb with a small 120 to 6v transformer connected to a constant voltage transformer, was found to elliminate the noise.

It was noticed that fatigue, drop of the output signal with time, was significant, but the cause was a faulty photomultiplier tube. Upon substitution of a new IP28 tube, the record from five hours of running the apparatus showed no fatigue.

The sensitivity can be adjusted by controlling the amount of light which strikes the tube, or by adjusting the voltage across the dyodes.

The output of the sixteen junction thermopile is recorded in a 0 to 1 mv., 0 to 21 mv., variable span Honey-

well recorder. The output of all the other measuring instruments is recorded in a Honeywell 12 point recorder with a converted span of 4 mv..

To measure the air stream velocity, and to calibrate the hot wire anemometer, a micromanometer described by Shedden (29) is used. Accuracies of $\mp$ 0.1 ft/sec are possible with the micromanometer. For measurements in the main stream, the impact probe is hypodermic tubing, stainless steel type 304, with 0.043in.O.D. and 0.027 in. I.D.. The boundary layer impact probe is made of 0.025 in. O.D. and 0.013 in. I.D. tubing. The boundary layer probe can be accurately positioned with a vice-like carriage fitted with a micrometer (see Shedden 29).

The turbulence intensity measurements are made with a Thermo-Systems, Inc., Model 1000 A, constant temperature heat flux system. The probes are Thermo Systems No. NT-12 fitted with SP2 (0.0002 in. Pt wire) , and ST1.5 (0.00015 in. Tungsten) hot wires. To calculate the turbulence intensity one requires the value of the root mean square of the fluctuating component of the power. The relation between the measured quantities and the turbulence is (see Thermo-Systems Technical Bulletin No.4, Ref.36):

$$\frac{\sqrt{\bar{p}^2/n}}{p - p_o} = \frac{\sqrt{\bar{u}^2}}{U_\infty} = \text{turbulence intensity} \quad ,,,,,(50)$$

p = average power level
p_o = average power level at zero velocity
$\sqrt{\bar{p}^2}$ = RMS value of the fluctuating component of power

n = constant which is a function of wire Re number

n = 0.45 if Re < 44 , n = 0.51 if Re > 44

The value of the average power level (P), can be read from the meter on the 1000 A Thermo Systems bridge. The value of P_o can be obtained from a calibration of the hot wire against the micromanometer and an extrapolation to zero velocity.

In order to obtain the root mean square of the fluctuating component, the output from the hot wire bridge is connected to a Ballantine 320 - S/2 True RMS Voltmeter. An auxiliary 2000 microfarad capacitor is used with the RMS meter to dampen the magnitude of the oscillations of the indicator needle.

A 545 A Tektronics oscilloscope, which receives the 1000 A Thermo Systems bridge power output, is used to indicate visually, the transition from a laminar to a turbulent boundary layer.

The Brooks frequency converter, The Ballantine RMS meter, and the 1000 A thermo Systems bridge, are rack mounted as shown in the picture, Fig. 2.

To position the hot wire, and to calibrate the optical profilometer, an Eberbach model 5100 cathetometer is used.

Expected error in measurements used to obtain the thermal conductivity.

The following table presents the most probable errors of the variables which have to be measured to calculate the thermal conductivity.

Table II

variable	expected error (%)	
mass flow rate	1	
coolant heat capacity	2	
coolant temp. diff.	1	
frost height	2	(at steady state)
$T_s - T_p$	2	(depends on the relative magnitude of the diff. $T_s - T_p$)
$T_\infty - T_p$	3	

To measure the heat leak, a teflon plate, 0.025 in. thick, is placed over the test plate surface. The total heat transferred to the coolant is measured. The teflon surface temperature, at the teflon-air interface, is measured with the radiometer thermometer. The amount of heat transferred through the teflon plate is calculated from known values of the heat transfer coefficient. The value of $q_{\text{heat leak}}$ is calculated by subtracting the heat flux through the teflon plate from the total heat transferred to the coolant with the plate on.

If one assumes that the errors in Table II represent the most probable errors in the measured variables, then the following probable error expected errors can be calculated.

Probable error in total heat transferred:

$$\text{p.e. in } q = \frac{\Delta q}{q} = \mp \sqrt{\left(\frac{\Delta m}{m}\right)^2 + \left(\frac{\Delta c_p}{c_p}\right)^2 + \left(\frac{\Delta (T_{out} - T_{in})}{(T_{out} - T_{in})}\right)^2}$$

$$= \mp \ 2\ \%$$

Probable in corrected heat flux:

$$\text{p.e. in } q_w = \frac{\Delta q_w}{q_w} = \mp \sqrt{\left(\frac{\Delta q_{w\ +\ \text{heat leak}}}{q_w}\right)^2 + \left(\frac{\Delta q_{\text{heat leak}}}{q_w}\right)^2}$$

$$\text{p.e. in } q_{\text{heat leak}} = \pm \sqrt{\left(\frac{\Delta q_{T \text{ with tef}}}{q_{\text{heat leak}}}\right)^2 + \left(\frac{\Delta q_{\text{tef}}}{q_{\text{heat leak}}}\right)^2}$$

assume: $q_{\text{heat leak}} = 1/3\ q_w$

$q_{\text{tef}} = 1/4\ q_{\text{heat leak}}$

substitution of numbers gives:

$$\text{p.e. in } q_{\text{heat leak}} = \pm \sqrt{(2 \times 5/4)^2 + (5 \times 1/4)^2}$$

$$= \pm 3\ \%$$

$$\text{p.e. in } q_w = \pm \sqrt{(2 \times 4/3)^2 + (3 \times 1/3)^2}$$

$$= \pm 3\ \%$$

Probable error in heat transfer coefficients:

$$\text{p.e. in } h_{\text{conv}} = \pm \sqrt{\left(\frac{\Delta q_w}{q_w}\right)^2 + \left(\frac{\Delta (T_\infty - T_p)}{(T_\infty - T_p)}\right)^2}$$

$$= \pm \sqrt{(3)^2 + (3)^2}$$

$$= \pm 4.2\ \%$$

Probable error in heat conductivities of frost:

$$\text{p.e. in } k_d = \pm \sqrt{\left(\frac{\Delta q_w}{q_w}\right)^2 + \left(\frac{\Delta h}{h}\right)^2 + \left(\frac{\Delta (T_s - T_p)}{(T_s - T_p)}\right)^2}$$

$$= \pm \sqrt{(3)^2 + (2)^2 + (2)^2}$$

$$= \pm 4.1\ \%$$

Description of experimental apparatus.

The cryogenic test plate is situated in the test section of a low velocity wind tunnel. With the present variable speed motor, velocities from 10 ft/sec to 50 ft/sec can be obtained. The air stream enters the test section through a square opening which measures 8 in. by 8 in.. The test section is 25 1/4 inches long and is followed by a 22 1/4 in. long section where the heaters are located. The air stream then passes through a blower and is recirculated back to the test section after it passes through a number of screens regulating fins, and a convergent section.

The heaters were redesigned so that they could supply 3000 Btu/hr, or about 1000 watts. Four strip heaters with fins are used.

The air temperature is controlled with a Yellow Springs Instrument Co. , model 63 RA, thermistemp controller. Temperatures around 90°F can be maintained constant to within $\mp$ 0.5 °F.

The humidity of the air stream is controlled by opening or closing a solenoid valve which allows 8 psig. steam to enter the heating section of the wind tunnel. The operator keeps close watch of the wet bulb temperature in the multiple point recorder and decides when to open or close the solenoid valve. The wet bulb temperature can be controlled to within $\mp$ 1 °F.

The test section of the wind tunnel is made of 3/8 in.

thick plexiglass and has a removable top and a side wall which opens to permit easy access to the test plate. An aluminum plate located in the lower part of the test section can be raised or lowered to control the pressure gradient. The top can also be raised or lowered.

While this project was under way, the tunnel location had to be changed. A great deal of care was taken to insure that it was reassembled properly. Measurements of the velocity and intensity of turbulence at various cross sections of the test section, showed that, for a zero pressure gradient, the velocity was constant to within $\mp$ 0.1 ft/sec. The intensity of turbulence, for a stream at 31.7 ft/sec, was 0.36 % and did not deviate by more than about $\mp$ 0.01 %.

The test plate is made with two pieces of 0.016 in. H.H. brass and one of 0.091 in. H. H. brass. The 0.091 in. piece has channels through which the coolant passes. One of the design requirements is that the maximum temperature difference between any two points on the plate, should be less than four or five degrees Fahrenheit. For the heat fluxes expected in this investigation, and with Freons as coolants, the test plate should be able to stand flow rates of 15 lb / min . Various unsuccesful designs were tried. The following design finally met the requirements:

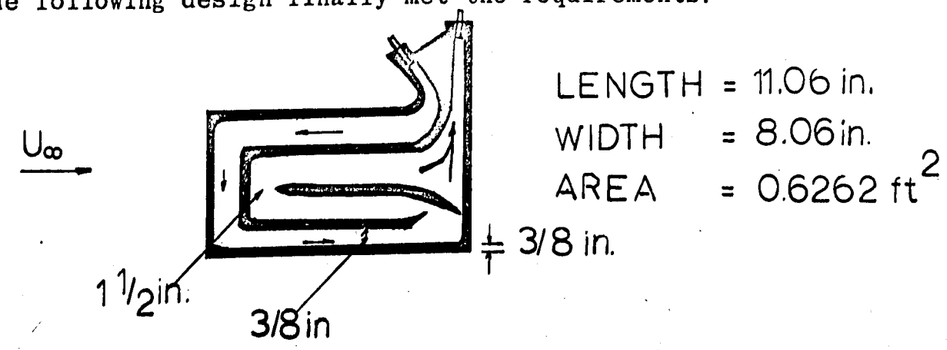

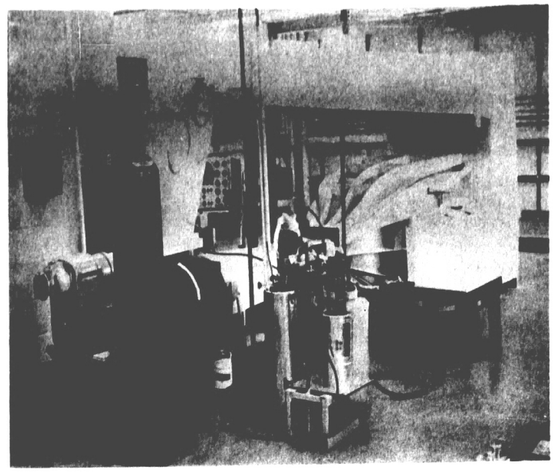

Fig. 4: Instruments on East Side

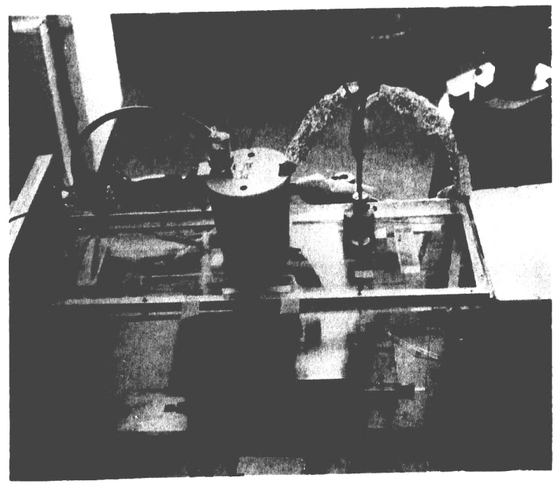

Fig. 5 : Test Section

The plate was soldered all at one time with the exception of the entrance 3/8 in. copper tubes. Eutector solder No. 157 PA was used. The plate was placed, pressed between two pieces of asbestos, in an oven at 550 °F for one hour. The adaptor from the flat plate to the copper tubes was made with four pieces of 0.091 in. H.H. brass which were soldered to the plate at the same time the plate was made. Then, the holes for the 3/8 in. copper tubes were drilled.

The plate sits in the tunnel test section over a plexiglass support which has a leading edge 4.06 in. long. The thickness of the support is 5/8 in. at the front of the brass plate. The total length of the support is 16.9 inches (see Fig. 5).

The test plate cooling unit must be able to maintain a constant plate temperature for about one to four hours. The coolant to the inlet of the plate must cover the range from 0°F to -250°F . An Eastern 60557, type 101, 1/8 Hp., pump, circulates the Freons from an insulated tank , 10, in. diameter and 21 in. tall, to a heat exchanger where the Freons are cooled by liquid nitrogen. From the heat exchanger, the coolant passes through the turbine flow meter and then to the test plate. One bypass is provided at the entrance to the plate, and another before the heat exchanger. The heat exchanger is a double helical coil through which the coolant flows. In the center of the helical coil is a finned tube through which liquid nitrogen flows. The coil and finned tube sit in a stainless steel, Hofman, 6 in. by 24 in. ,

dewar, which is 3/4 full with Freon and is agitated with a Lightnin mixer model L, whose speed is controlled with a powerstat. The rate of flow of coolant is also controlled with a powerstat connected to the pump. The rate of flow of liquid nitrogen is controlled by two solenoid valves. One of the valves admits nitrogen gas to the liquid nitrogen dewar. The other solenoid valve deppresurizes the dewar when it is opened. Both valves are controlled by the operator from the control pannel.(see Fig.4).

Operating procedure.

The wind tunnel motor is started one hour before the coolant is passed to the plate. At the same time that the tunnel is started, the heaters and thermistemp controller, the steam, the hot wire bridge, the RMS meter, the flow indicator, the oscilloscope and the optical radiometer are turned on.

About fifteen minutes before the start of the run, the radiometer is checked against the ice point. If the deviation is large, more than two degrees, the gain screw inside the instrument is adjusted to zero. If the deviation is small, then, one simply notes its magnitude and then corrects the data.

A two millivolt span is set on the Honeywell recorder, and the zero point is checked with the input terminals shorted.

The calibration frequency of the flow meter is checked and adjusted if necessary. This calibration hardly ever re-

quires adjustment.

About five gallons of Freon are poured into the dewar. In the temperature range between 0°F and -100°F, Freon 11 is used. At lower temperatures, Freon 12 will be used.

The valve to the main heat exchanger is closed. The Freon will now flow through a coil in a bath, where it will be precooled by liquid nitrogen until a temperature about 20°F lower than that of the desired plate temperature is obtained. Thermocouples which are located in all the baths are monitored in the multiple point recorder. When the coolant has been precooled to the desire temperature, the pump is stopped, and the valve which leads to the main heat exchanger is opened. The valve on the exit of the heat exchanger is closed and a valve which allows the Freon to flow into the exhanger dewar is opened. When the dewar is 3/4 full, the pump is stopped and the valve which allows Freon to the dewar is closed. The exit valve of the heat exchanger is now opened.

The teflon plate is placed over the test plate surface. The valve at the exit of the plate must be opened.

A great deal of care must be taken at this point so that the turbine meter and the test plate do not receive the impact of a fast moving stream. To prevent this, the speed of the pump is slowly increased with the powerstat located in the control pannel.

Once the freon is flowing through the plate, the steam solenoid valve can be opened until the desired humidity is

reached.

A pressure of 5 psig should be kept in the liquid nitrogen dewar. the rate of liquid nitrogen to the exchanger is controlled with the solenoid valves which determine the dewar pressure.

When the plate termperature which is desired has been reached, the plate temperature is maintained constant by regulating the rate of liquid nitrogen to the exchanger. When the plate temperature is constant, the required variables are recorded.

The teflon plate is now removed from the test surface and frost will immediately start to deposit. A continuous record of the variables is kept. The humidity of the air stream, the flow of coolant, and the plate surface temperature must be continuously watched and controlled.

Periodically, measurements of height with the cathetometer, and measurements of turbulence intensity can be made.

To measure the deposit density, the air flow is stopped. and the test section is opened. A 1/4 inch thick teflon strip, which has a cut one inch wide by 11 inches long, is placed over the frost. The frost which is inside the slit is scraped with the teflon spatula. The scraped frost is immediately placed inside small flasks and weighed.

To end the run, the pump is stopped, the Freon transferred to its container, the nitrogen gas regulator valve is closed, and all instruments, except the recorders,are

turned off. Care must be taken, before leaving the laboratory, to insure that the heaters and the solenoid valves are off.

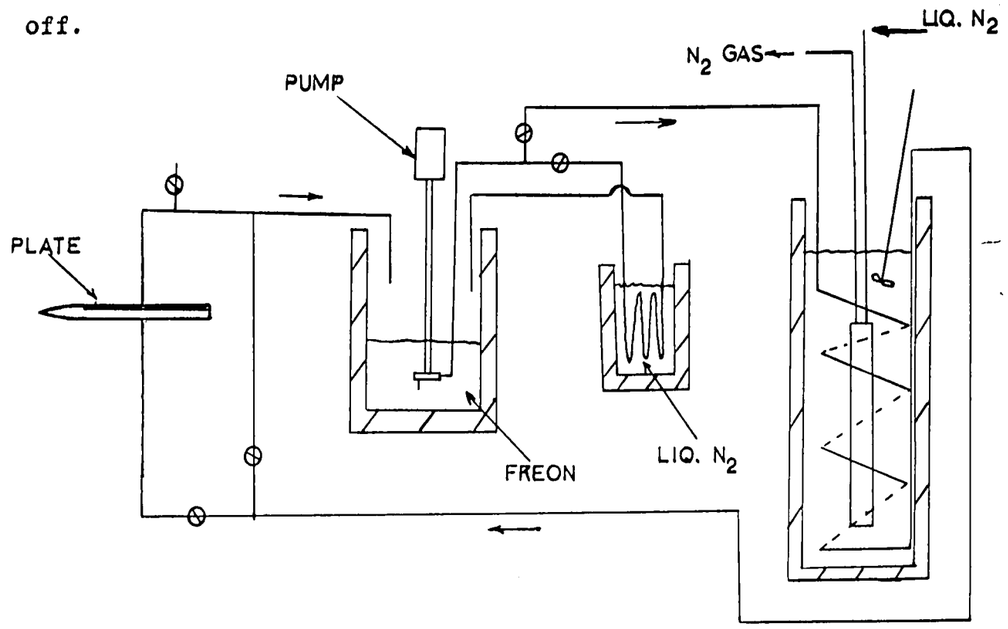

FIG.6: FLOW DIAGRAM

Discussion of results.

One of the first steps in this investigation was to determine the accuracy of the experimental frost thermal conductivities.

Most of the instruments which are used to measure, have their own standardizing circuits and their accuracy can be trusted to meet the manufacturers specifications. The radiometer-thermometer, and the micromanometer, do not have standardizing circuits.

Micromanometers are generally regarded as primary standards. Nevertheless, to check the micromanometer, boundary layer velocity distributions were measured with the impact tube. If the well known laminar velocity distributions did not agree with the ones measured in this study, then one could suspect the micromanometer. It was expected that the slight curvature of the leading edge would introduce some small deviation from the theoretical distributions.

The results from Fig.8 , indicate that the measured turbulent boundary layer velocity distribution agrees very well with that of other observers. The laminar boundary layer curves are also, very close to the theoretical curve, as can be seen in Fig. 7.

The laminar boundary layer velocity distribution which was measured with the hot wire, is closer to the theoretical distribution than that measured with the impact tube. Since the hot wire was calibrated with the micromanometer, one may

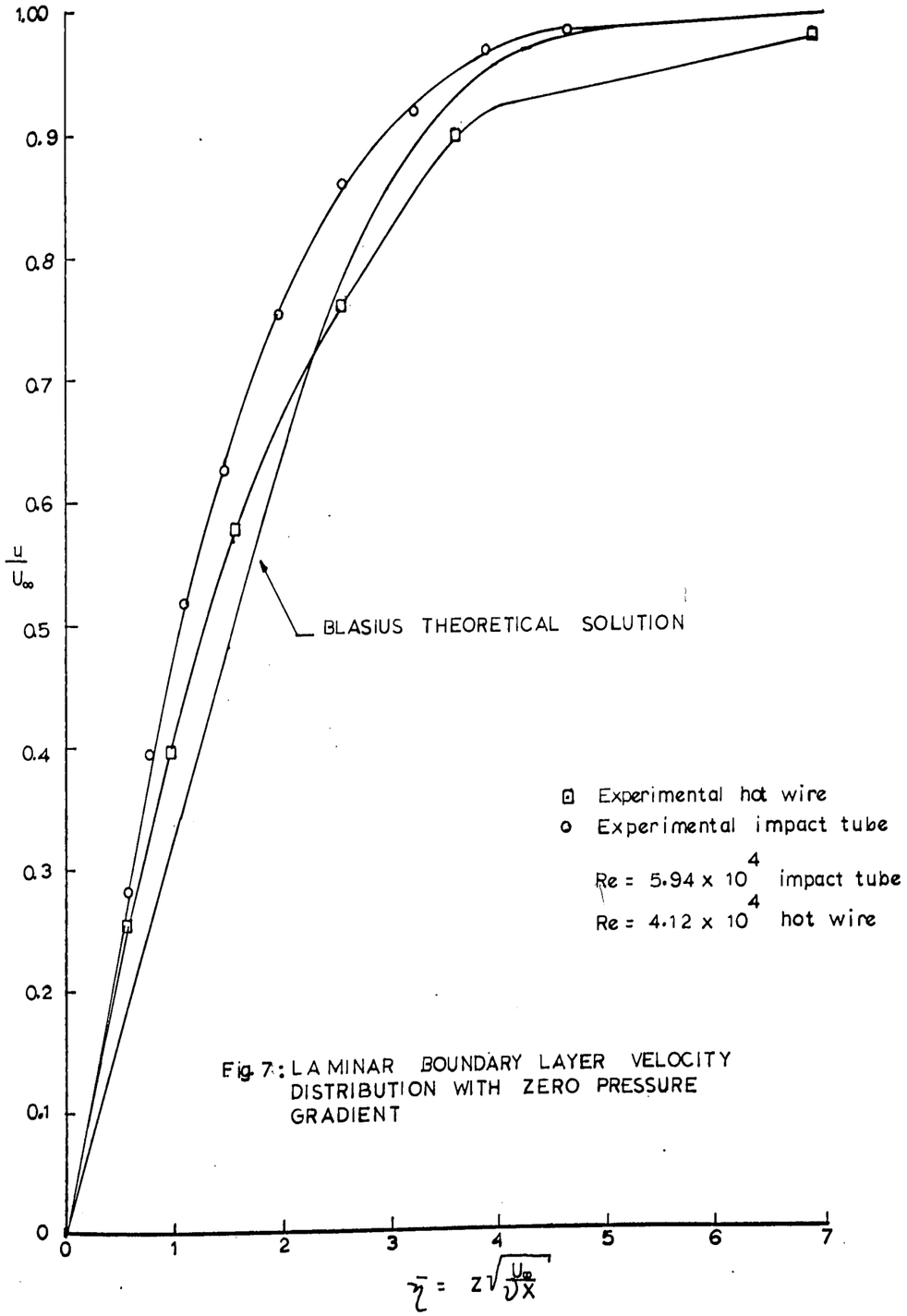

Fig 7: LAMINAR BOUNDARY LAYER VELOCITY DISTRIBUTION WITH ZERO PRESSURE GRADIENT

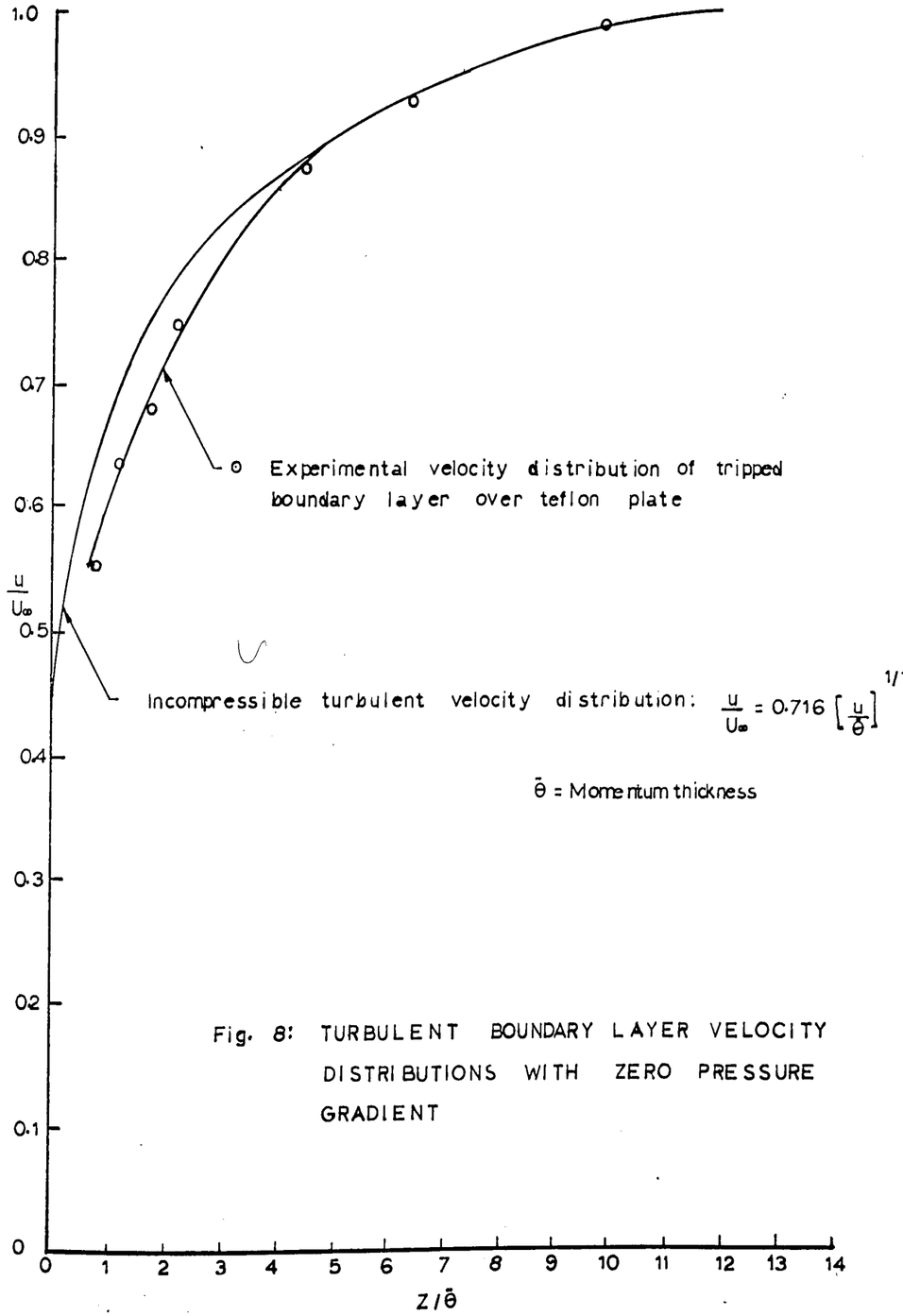

Fig. 8: TURBULENT BOUNDARY LAYER VELOCITY DISTRIBUTIONS WITH ZERO PRESSURE GRADIENT

suggest that the larger error obtained with the impact tube, is due to the relatively large size of the impact tube diameter compared with the laminar boundary layer thickness.

Fig. 9, compares the velocity distribution over the teflon plate with the Blasius laminar boundary layer distribution. The distribution over the teflon plate has a much steeper slope near the plate than does the Blasius profile. Also, the boundary layer thickness is much greater over the teflon plate than that corresponding to a laminar boundary layer. One concludes from Figures 8 and 9 , that the boundary layer over the teflon plate is turbulent, or very advanced transition.

The pictures in Fig. 10, were taken with the hot wire inside the boundary layer. Picture (a), corresponds to the laminar boundary layer profile shown in Fig.7 . Picture (b) , tends to confirm that the boundary layer over the teflon plate is turbulent. To insure that the boundary layer would be turbulent in all cases, a tripping wire was placed at the leading edge of the teflon plate. Tests with the hot wire showed that the same characteristics of picture (b) are observed , within the teflon plate boundary layer, throughout the whole free stream velocity range.

The heat transfer coefficient, without frost deposition, was measured over a range of Reynolds numbers. The plate surface temperature was kept above the dew point of the air stream so that no heat was transferred by condensation.

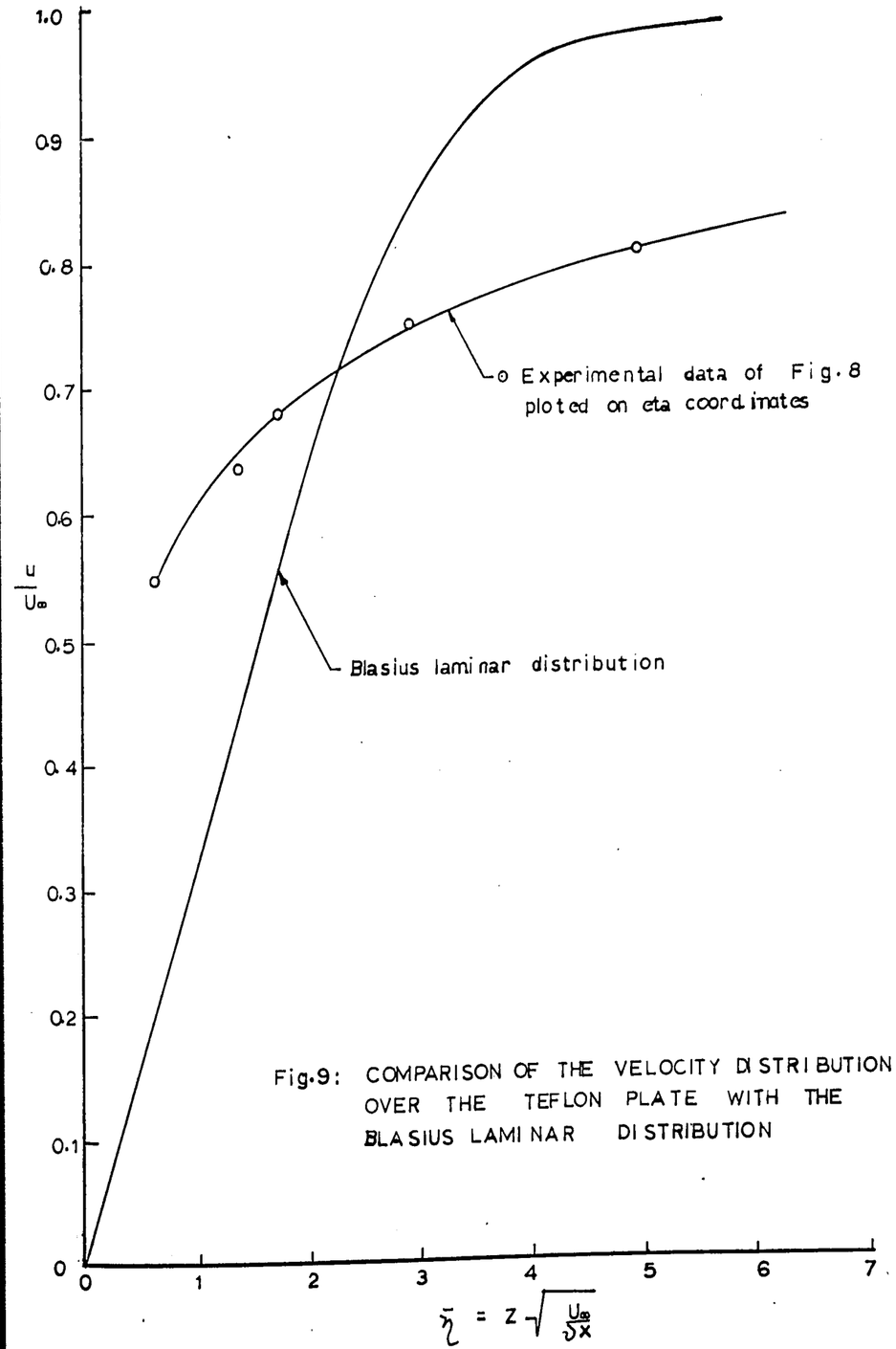

Fig.9: COMPARISON OF THE VELOCITY DISTRIBUTION OVER THE TEFLON PLATE WITH THE BLASIUS LAMINAR DISTRIBUTION

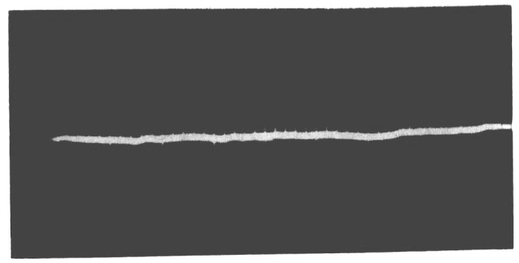

Picture (a) : Hot-Wire in Test Plate Boundary Layer

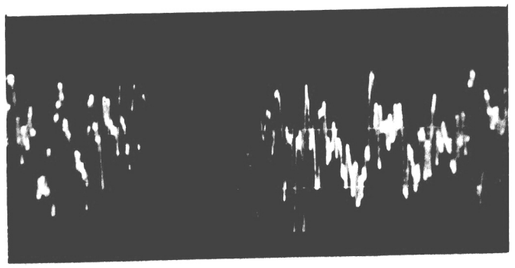

Picture (b) : Hot-Wire in Teflon Plate Boundary Layer

Fig. 10: Pictures of Turbulence Characteristics Within the Boundary Layer

Measurement of heat transfer coefficients involves the following steps:

1. Measurement of the total heat transferred to the coolant with the teflon plate on.
2. Calculation of the heat transferred through the teflon plate; calculation of heat leak.
3. Measurement of the total heat transferred to the coolant without the teflon plate on.
4. Calculation of the heat transfer coefficient; calculation of Nusselt numbers.

The only measurement which does not have to be made to measure heat transfer coefficients but which is made when one measures the frost thermal conductivities, is the measurement of the height of the deposit.

The measured heat transfer coefficients can be compared with theoretical and well tested correlations of heat transfer coefficients.

Fig.11, shows that the measured values deviate by a maximun of $\mp$ 10 % from the laminar correlation. The most probable error in the Nusselt numbers is $\mp$ 3.4 %. The transition region falls in the same range of Reynolds numbers as given by Schlichting (28). The maximun Reynolds number which could be attained over the test plate was 2.5×10^5. Thus, no values of the Nusselt number could be obtained in the turbulent regime.

Fig. 11 also shows that the curved leading edge has a negligible effect on the flat plate characteristics.

When the total heat fluxes were calculated, it was found that the temperature difference between the inlet and

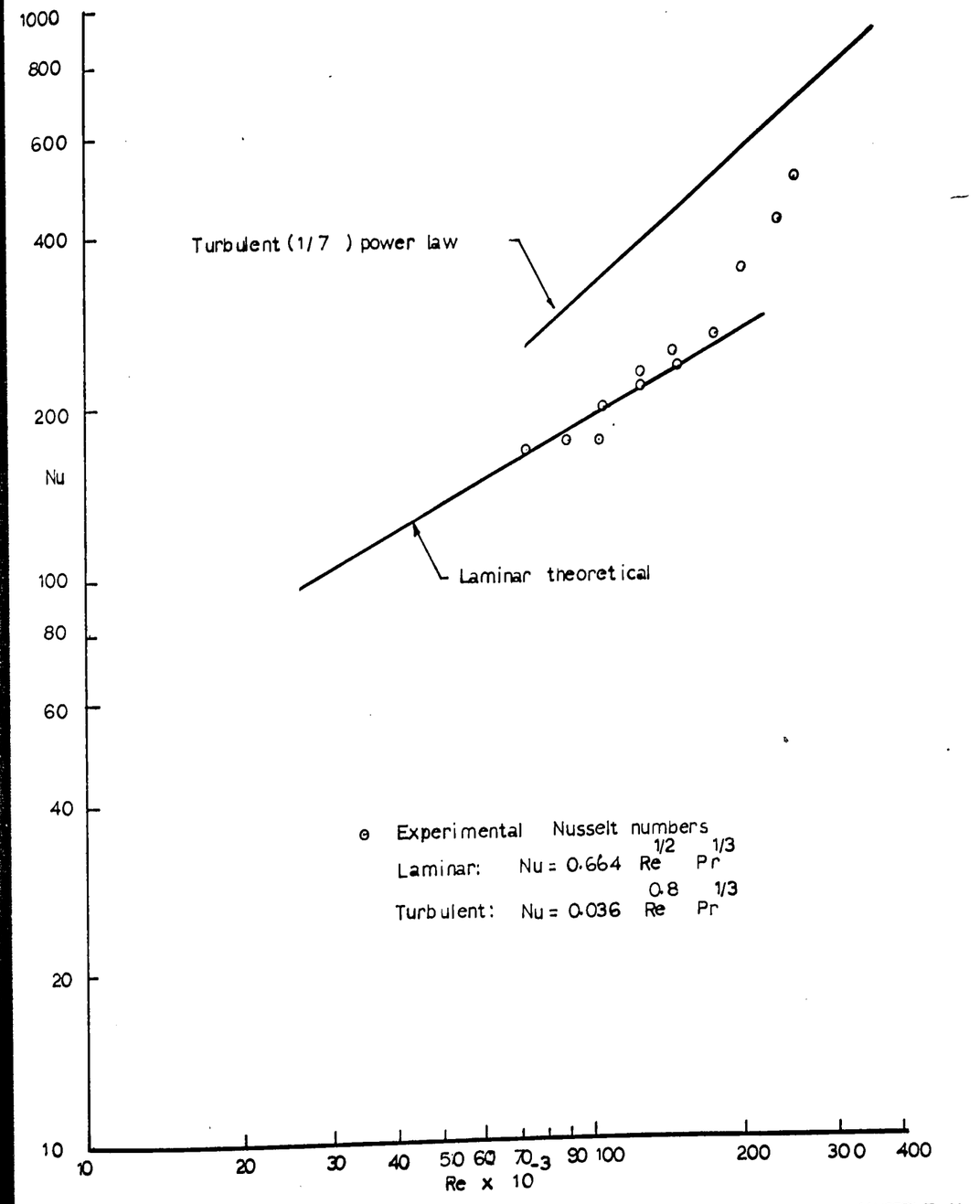

Fig. 11 : COMPARISON OF EXPERIMENTAL AND THEORETICAL NUSSELT Nos. WITHOUT FROST DEPOSITION

outlet streams of coolant to the plate was very sensitive to small deviations in the temperature of the inlet stream. The dynamic response of the test plate is similar to that of a shell and tube heat exchanger. The record of the temperature difference measured by the coolant thermopile, shows that the temperature difference varies sinusoidally with time. The sinusoidal response of the thermopile is caused by a sinusoidal change with time of the inlet coolant temperature. The inlet coolant temperature can be controlled to within $\pm$ 0.8 °F.

If the inlet coolant temperature changes very rapidly, the outlet temperature will lag. The temperature differences which were used to calculate the heat fluxes, were the average of the maximum and the minimum temperature differences in a given cycle. Note that the heat fluxes without frost deposition are smaller than the heat fluxes when frost deposits. Thus, one would expect that for the same flow of coolant, the relative error introduced by the sinusoidal change in the coolant inlet temperature, will be smaller when heat fluxes are measured with frost deposition. The largest error in measurement is caused by the changes in the inlet coolant temperature, and the lag in the response of the exit stream temperature.

Figures 12, 13, 14, and 15, show how the heat flux through the frost deposit varies with time.

In Fig. 12, the boundary layer remains laminar during

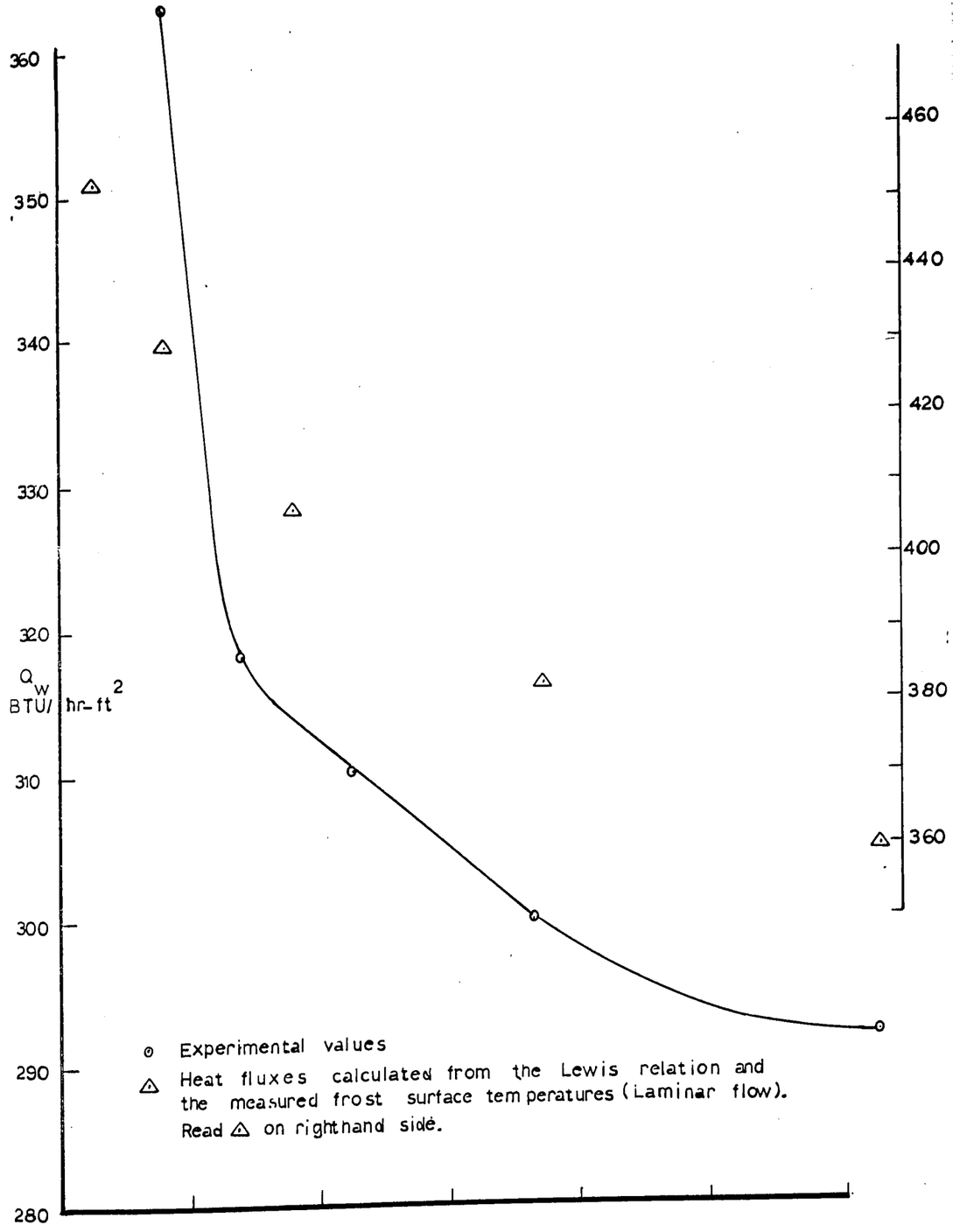

Fig. 12: TOTAL HEAT FLUX VERSUS TIME FOR RUN AT 28% R.H., 21.6 ft/sec, and T_p = - 20°F

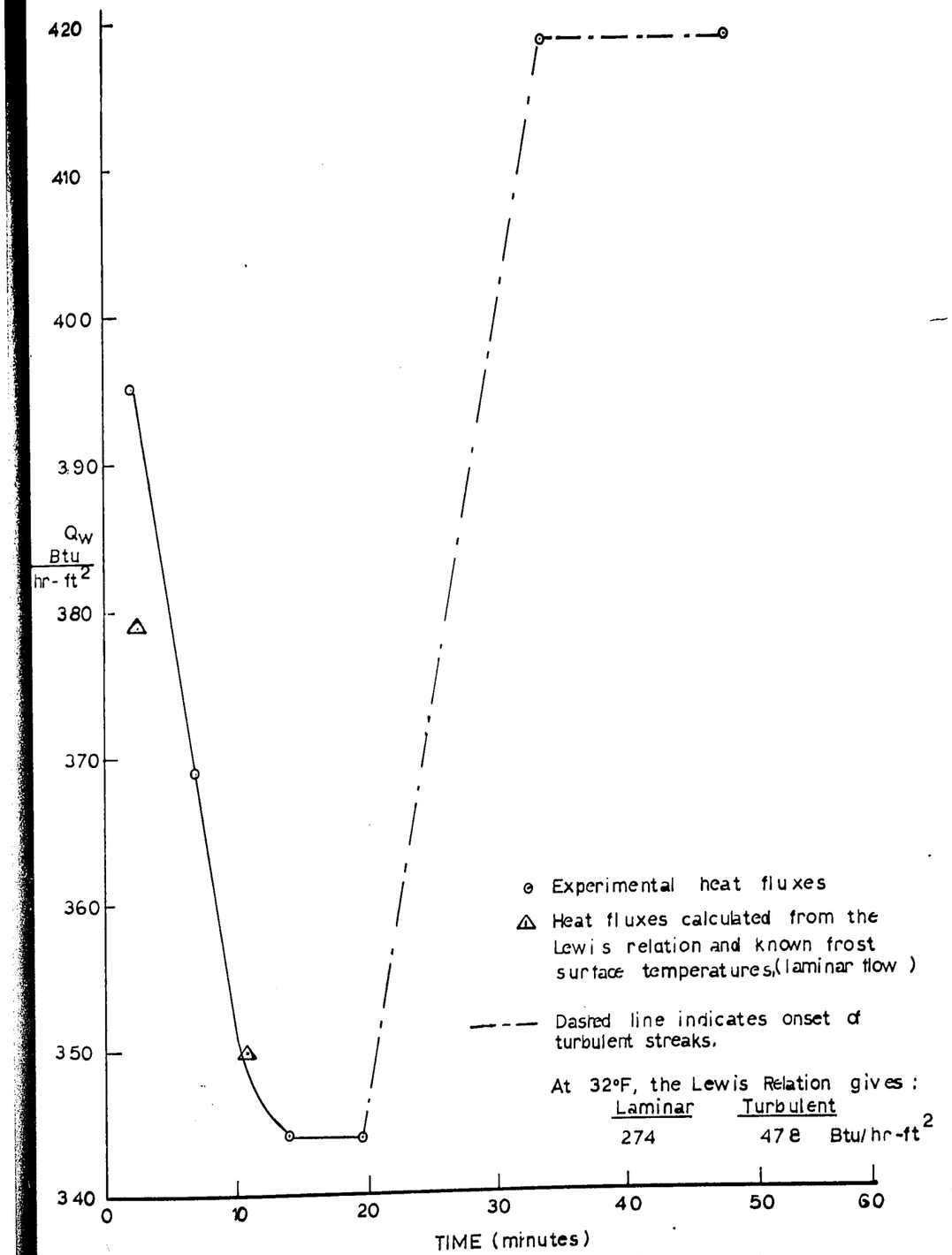

Fig.13: TOTAL HEAT FLUX VERSUS TIME FOR RUN AT 38% R.H., 21.6 ft/sec , T_p = 13°F

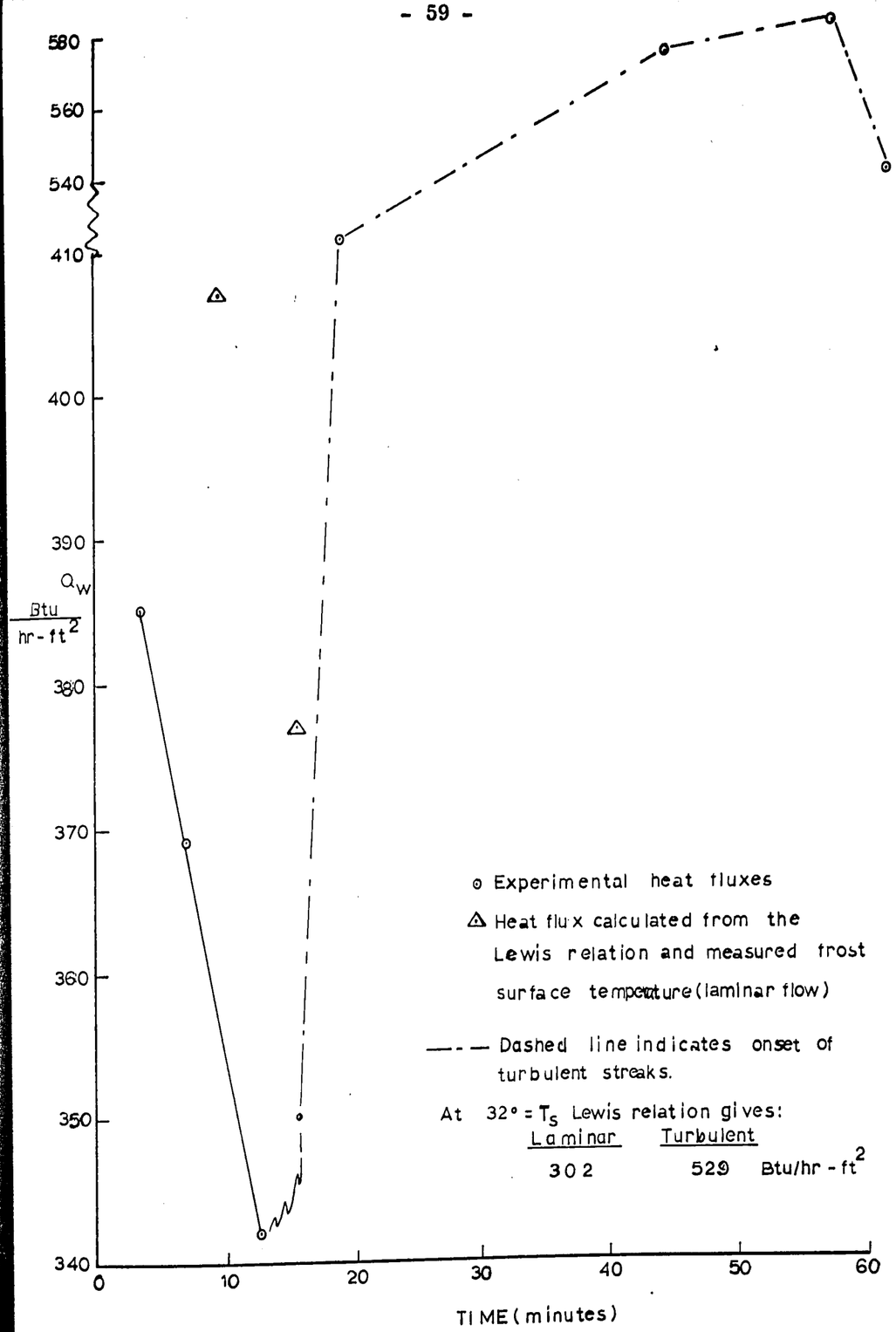

Fig. 14: TOTAL HEAT FLUX VERSUS TIME FOR RUN AT 21.6 ft/sec, 46% R.H., T_p=-18°F

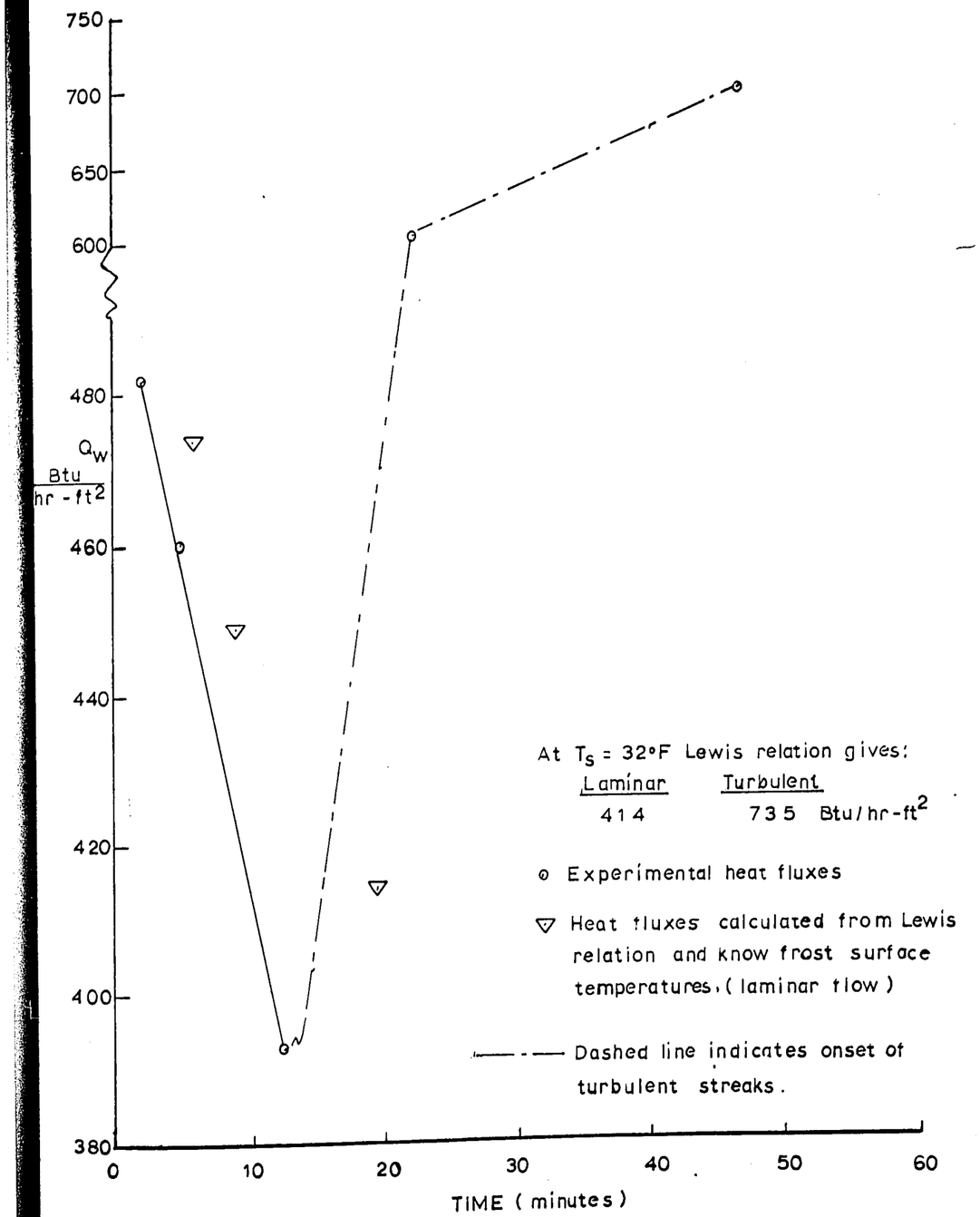

Fig.15: TOTAL HEAT FLUX VERSUS TIME FOR RUN AT 70% R.H., 21.6 ft/sec , T_p = -19°F.

the whole length of the run. The frost surface temperature, for this low free stream humidity, reached only 10 °F when the run was stopped after 76 minutes of deposition. The values within the triangles in Fig. 12, are heat fluxes calculated from the Lewis relation and the measured frost surface temperatures which are shown in Fig. 16. Note that the Lewis relation over-predicts the heat fluxes by as much as 20 % in this run.

The runs shown on Figures 13, 14, and 15, were made at the same free stream velocity as that of Fig. 12, but at higher free stream humidities. In all of these runs, as opposed to that of Fig. 12, the boundary layer was tripped after the frost reached a certain height. Turbulent streaks which were clearly visible because they changed the porosity of the deposit, appeared after the frost reached the critical height. When the hot wire was placed within the boundary layer on top of the streaks, a turbulent signal was observed in the oscilloscope. It did not take very long before the first few turbulent streaks grew and the boundary layer, over the whole frost surface, became turbulent. Note the sharp rise in the heat flux when the boundary layer becomes turbulent. The Lewis relation over-predicts the heat fluxes by about 10 % in this relatively high humidity runs.

In all cases, after the frost surface temperature reached 32 °F, a cyclic change of the deposit surface temperature was noticed. The surface temperature oscillated between about 28°F

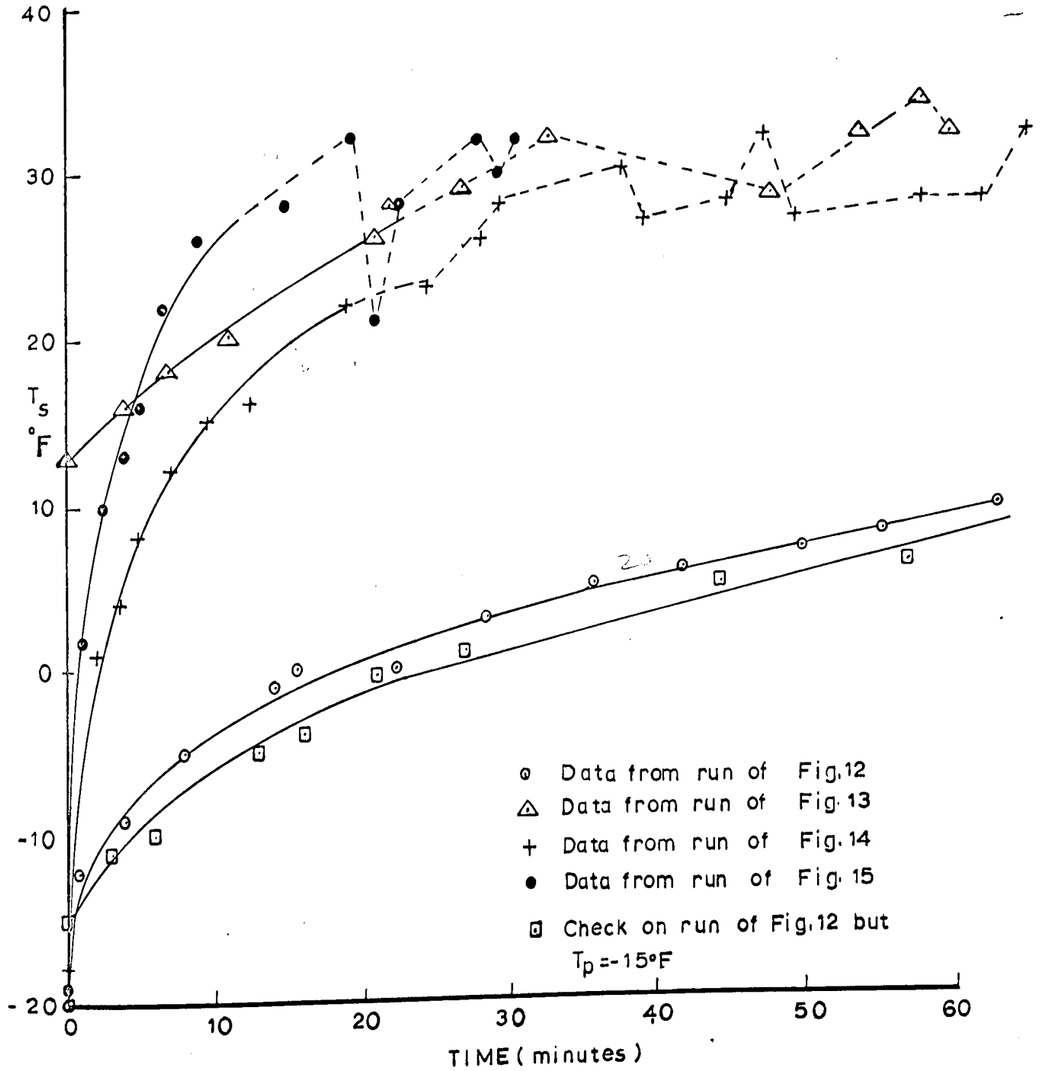

Fig. 16: FROST SURFACE TEMPERATURE VERSUS TIME

and 33°F.

Tests with the hot wire within the tripped boundary layer showed that, for the first 1/4 of an inch from the leading edge of the frost deposit, the boundary layer seemed laminar. Then, as the hot wire was moved downstream, signals characteristic of transition could be observed on the oscilloscope, and after about one inch from the leading edge, the boundary layer appeared to be completely turbulent. In all runs, a zero or slightly negative pressure gradient was maintained over the test surface. No evidence of separation of the boundary layer could be observed.

As can be seen from Fig. 17, there is a very well defined height after which the boundary layer becomes turbulent. It was found that the constant in Eq.(48) was too low. The following equation was found to give the critical height for the frost surface temperatures of this investigation:

$$\frac{U\,k}{\nu} \geq 1200 \qquad \text{.....(51)}$$

where:
U = Free stream velocity
k = Critical height
ν = Air kinematic viscosity

Fig. 18, indicates that the relation between frost surface temperature and height is non-linear, or at least, non-linear after a certain frost surface temperature has been reached. More data at other plate temperatures is needed to substantiate this conclusion.

Figures 20 and 19 will be discussed in relation to the

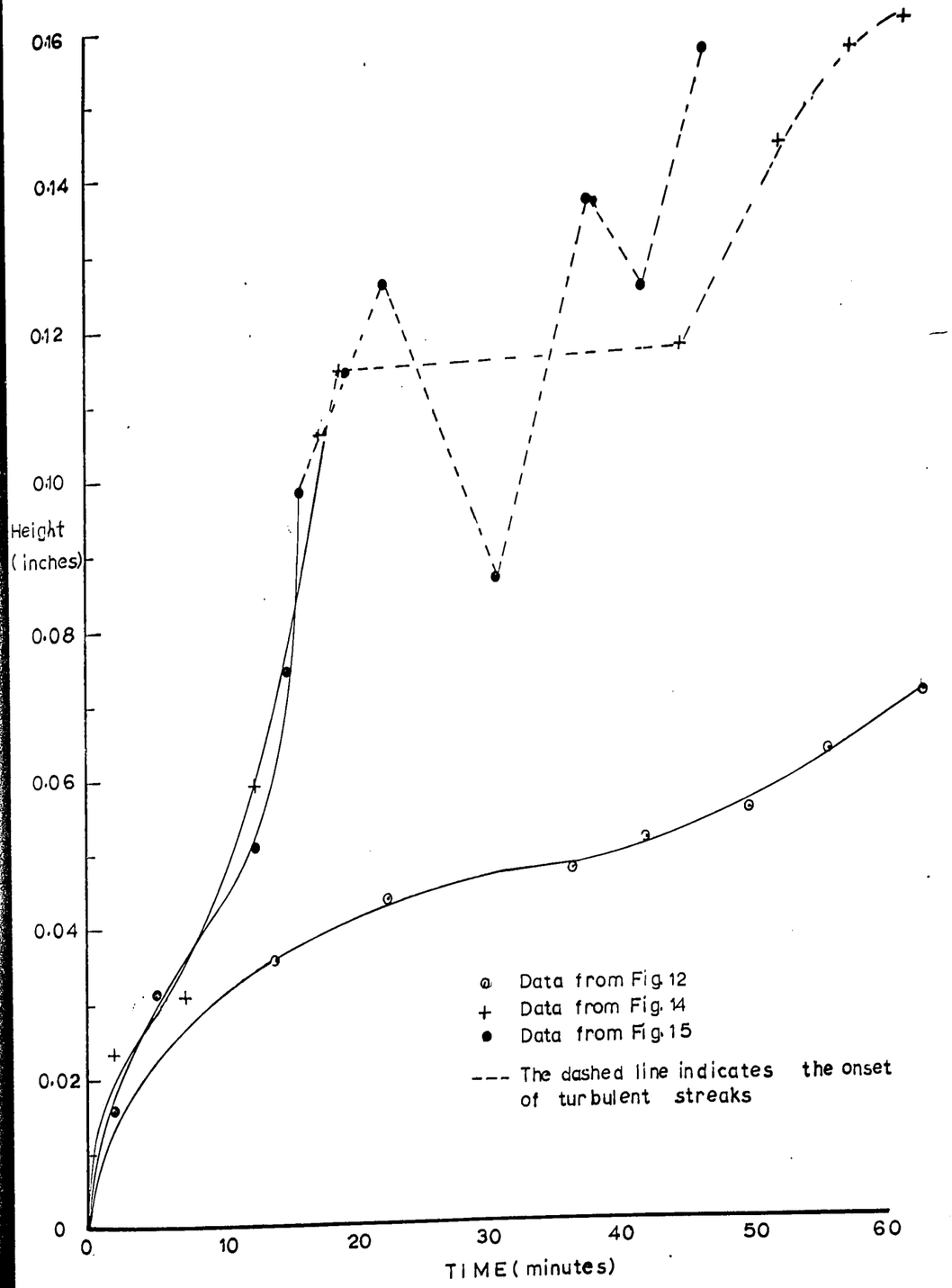

Fig.17: FROST HEIGHT AS A FUNCTION OF TIME

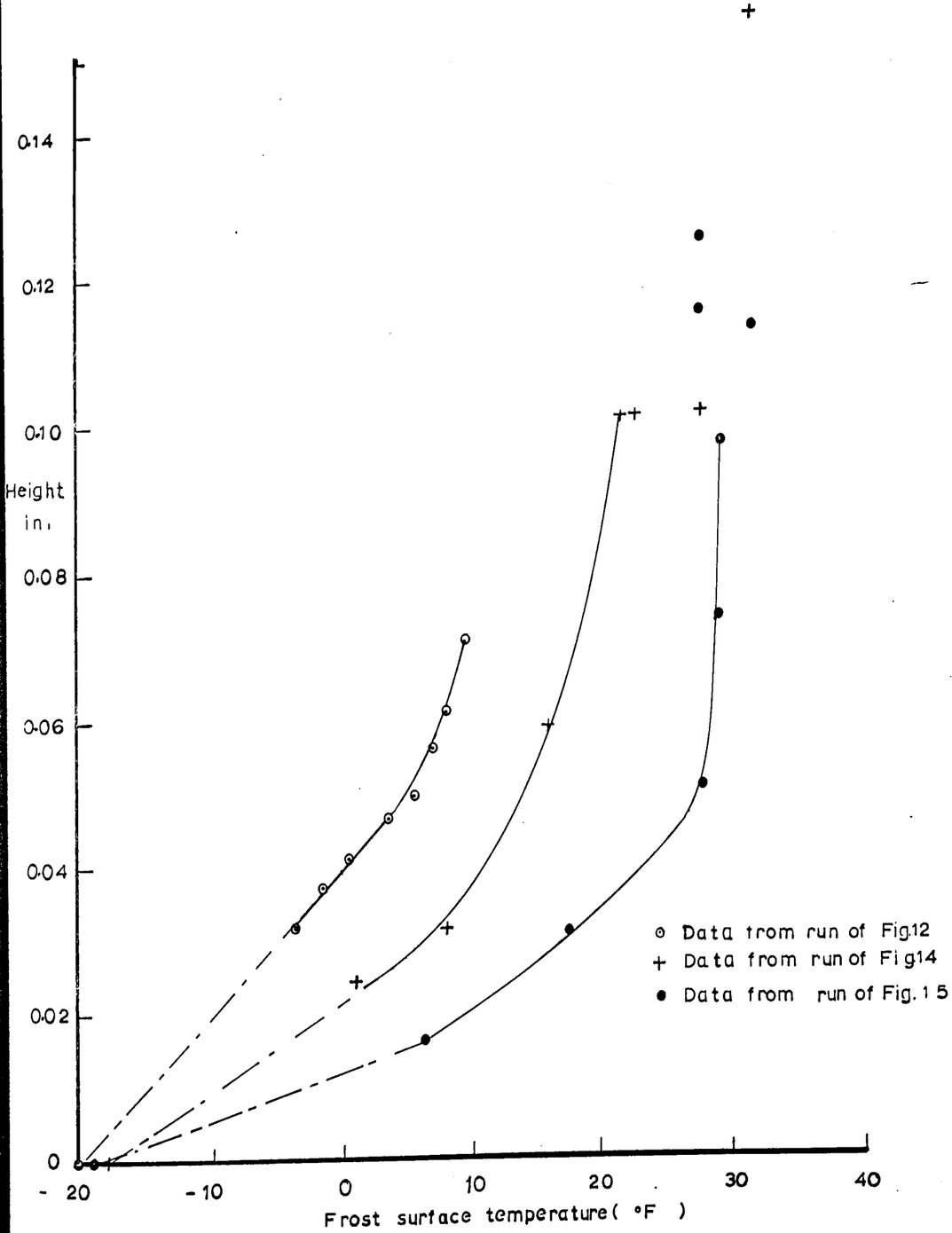

Fig.18: Relation Between Frost Surface Temperature and its Height

theory presented om pages 21 and 22.

The first effect predicted by the theory is that the desity, or the thermal conductivity, will increase at the very beginning of deposition until the clusters grow large enough to cross link and form a pattern of growth for the crystals. The data from the run shown on Fig.13, tends to confirm the first prediction as can be seen in Figures 19 and 20. Notice that the curve for the run of Fig.13, has a negative slope as one approaches zero time. At the beginning of deposition, the thermal conductivity of the deposit corresponds to the thermal conductivity of air. Since the thermal conductivity of air is smaller than the frost conductivity of run 13, and since the slope of the curve is negative near zero time, one concludes, that a maximum must occur on the thermal conductivity curve at a time very close to zero.

The curve of run 13, also shows the minimum caused by a decrease in the impingent heat mass flux and the increase in the internal diffusion of water vapor predicted by theory. Runs 14 and 15, reached a high frost surface temperature so rapidly that the diffusion effect predominates and only an increase of conductivity with time can be observed (see Fig.17).

Note that the thermal conductivity rises sharply when the boundary layer becomes turbulent. The points on Figures 19 and 20 that are not connected with lines cor-

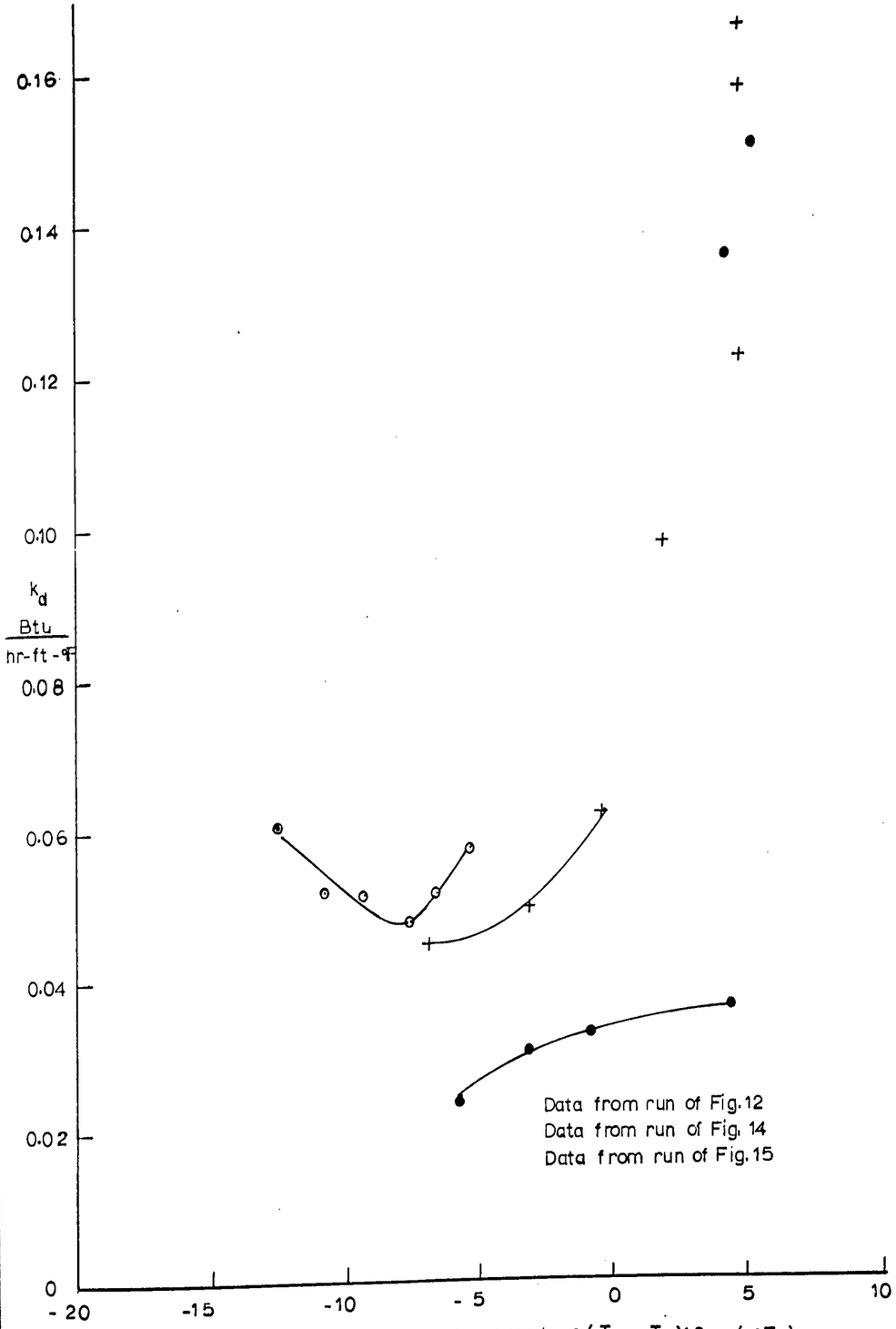

Fig.19: FROST THERMAL CONDUCTIVITY AS A FUNCTION OF ITS AVERAGE TEMPERATURE. EFFECT OF FREE STREAM HUMIDITY.

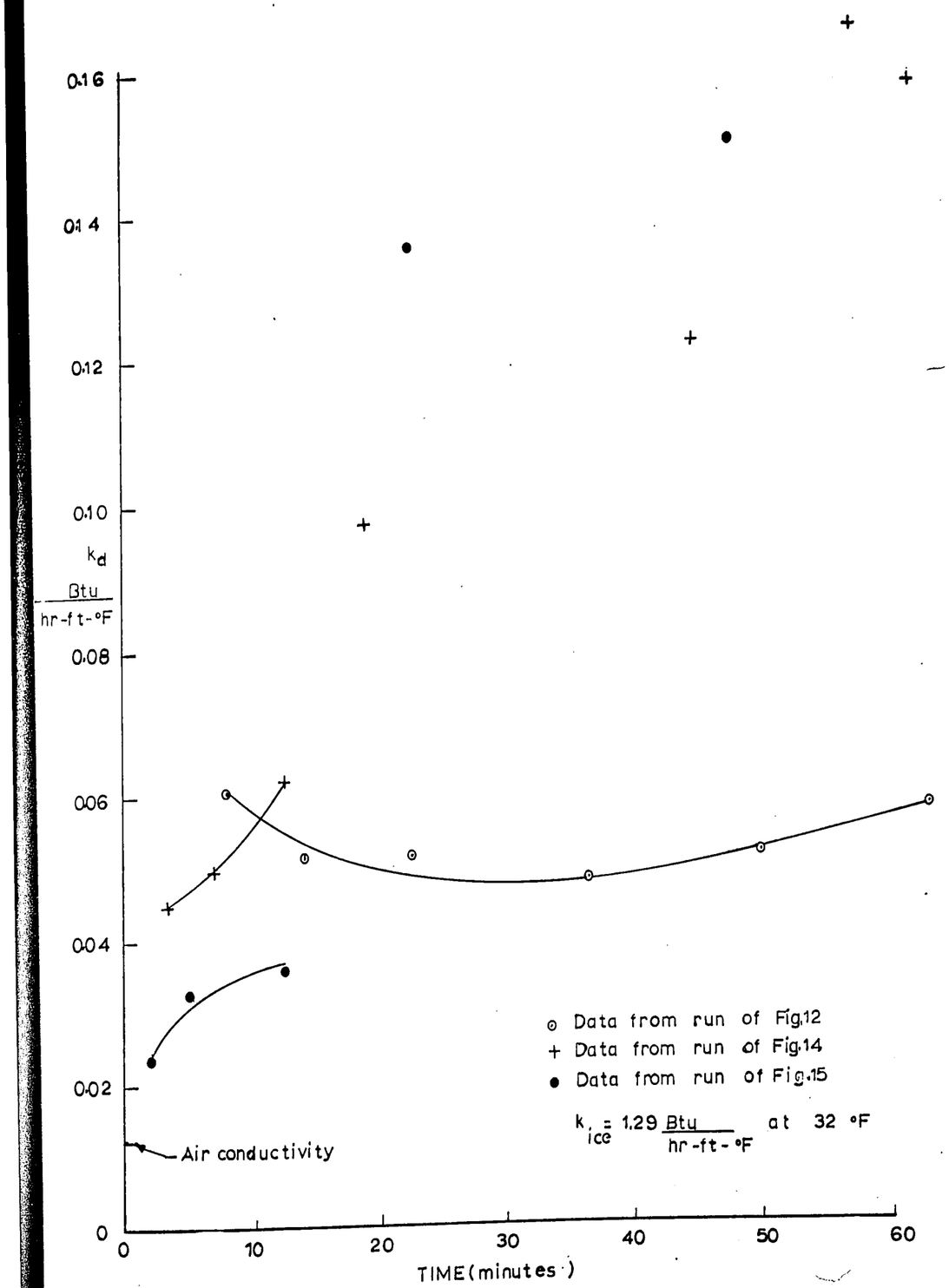

Fig. 20: THERMAL CONDUCTIVY OF FROST AS A FUNCTION OF TIME

respond to a turbulent boundary layer.

Two important questions have to resolved before one can correlate the measured average frost thermal conductivity with an average frost density. The first question is:

" What is the height distribution along the length of the plate surface ?" The observations up to the present time, indicate that there is no significant change in height along the length of the plate except for the initial 1/4 inch or so, where the deposit rises smoothly from zero to a constant heigth. When the boundary layer becomes turbulent, a slight dip is noticed at about one inch from the front edge of the deposit.

The second question to be resolved is:

" What is the frost density distribution along the plate ?" Since the mass transfer coefficient is a function of distance, it varies as the length to the - 1/2 power for laminar flow, and the height has been observed to be constant, then one would expect that the density should decrease from the front towards the back of the deposit. For laminar flow, one would expect that the density would vary approximately with the length to the - 1/2 power. The data of Fig. 21, indicates that the density varies approximately with the length to the - 1/2 power.

Figure 22 shows how the thermal conductivities and frost densities obtained in this investigation, compared with the values given for packed snow near 32°F by Devaux and Van Dusen (11), and some experimental values of Coles(11),

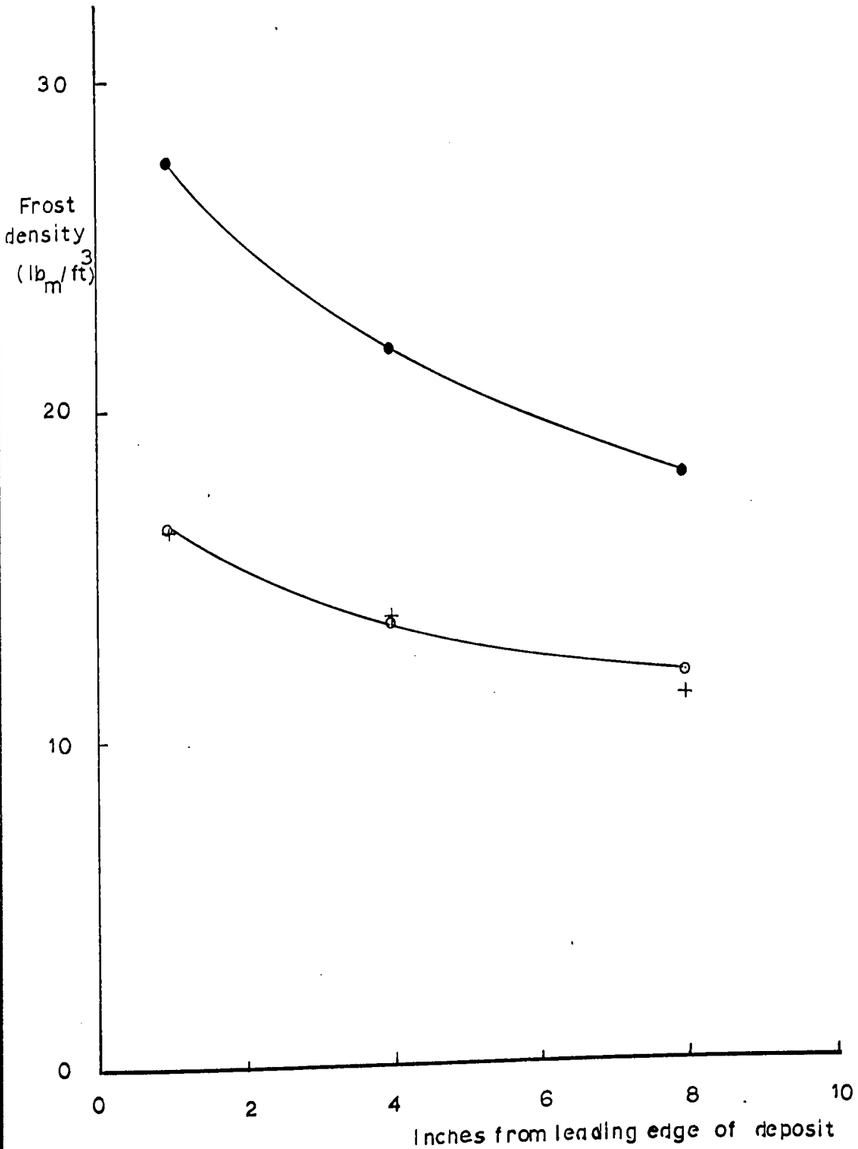

Fig. 21 : FROST DENSITY DISTRIBUTION ALONG THE LENGTH OF THE PLATE

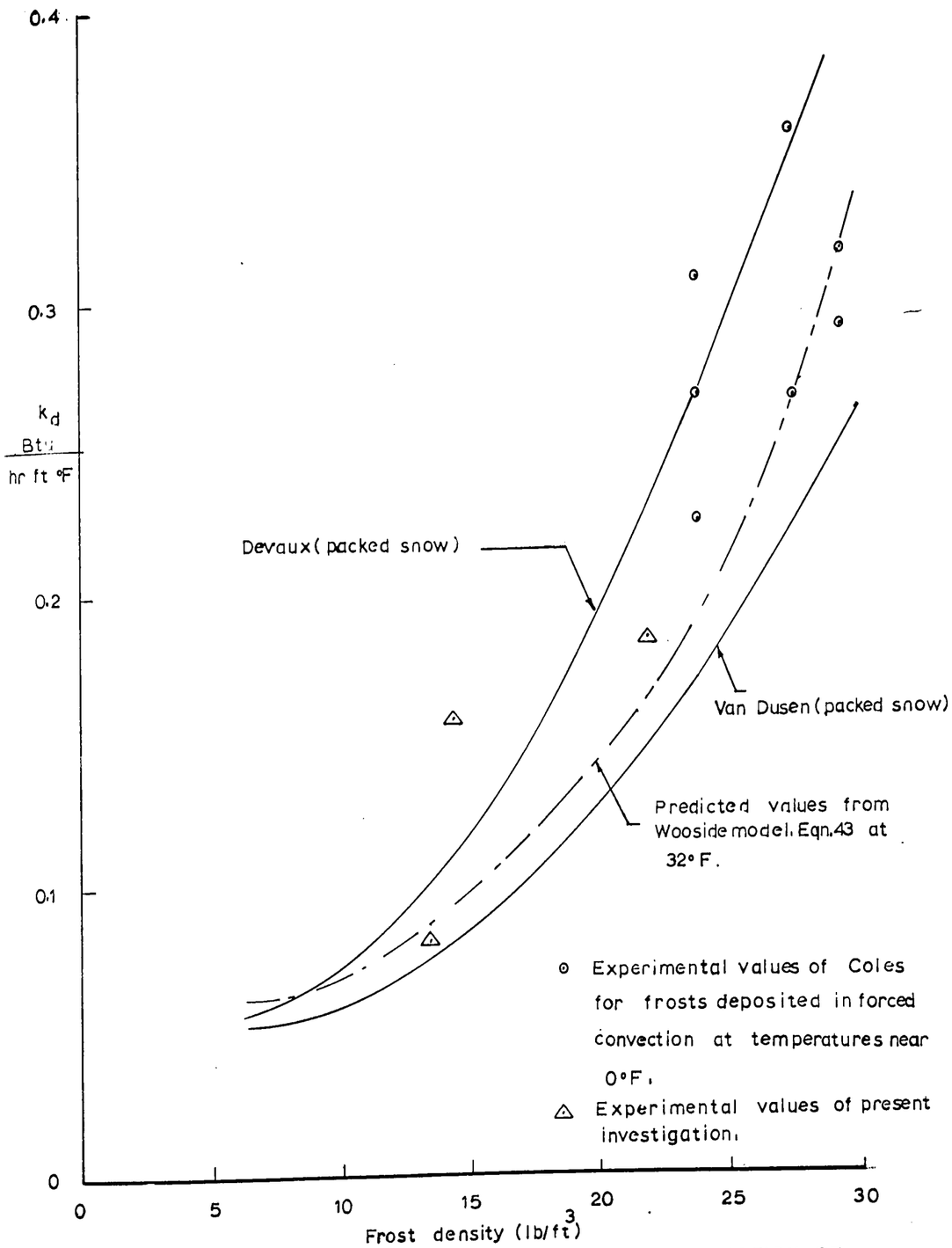

Fig. 22: FROST THERMAL CONDUCTIVITY AS A FUNCTION OF FROST DENSITY FOR TEMPERATURES NEAR 0°F

for frosts deposited in a forced convection stream at average temperatures near 0°F. The dashed line was calculated from Eq.(43) based on the Woodside model (41), for an average frost temperature of 32°F.

More data is needed to draw definite conclusions, but it appears that the Woodside model will correlate frost thermal conductivity and frost density data very well.

In future measurements of the frost thermal conductivity and frost density, the run will be stopped before the frost surface temperature reaches 32°F, because once water starts to form over the frost surface, measurements of height and surface temperature become more difficult. The point in Fig. 22, which falls out of the Devaux - Van Dusen curves, could be in error because of the difficulty in measurements when the frost surface temperature reaches 32°F.

Conclusions

1. Heat fluxes and heat transfer coefficients without frost deposition can be measured to within the expected limits of error.
2. The thermal conductivities and densities of frosts which deposit in forced convection conditions near 0°F, can be correlated by the theoretical model of Woodside (41), and the values of these properties are very close to those for packed snow near 32°F. More data is needed to substantiate this conclusion and to test the validity of the model at lower temperatures.
3. At a given frost average temperature, the thermal conductivity of frosts which form in a low humidity stream is higher than the thermal conductivity of frosts which form in a high humidity stream. More data is also required to substantiate this conclusion.
4. The height of the frost deposit is constant after about 1/4 inch from the front edge of the deposit.
5. The density of a deposit which forms in a laminar boundary layer, varies as the length to the - 1/2 power.
6. The assumption made by Libby and Chen(23) in their theoretical analysis, that the deposit surface temperature, at the frost-air interface, is constant with time, is incorrect.
7. The theory proposed in this investigation predicts qualitatively the growth of the deposit and the change of thermal conductivity and density with time.

8. The relation between the frost surface temperature and it height appears to be non-linear.

9. A critical height after which the boundary layer becomes turbulent is given by:

$$\frac{U_{\infty}\, k}{\nu} \geq 1200 \qquad \text{.....(51)}$$

for the frost surface temperatures encountered in this investigation.

10. The condition of minimum heat flux may not occur at the quasi-steady state because the boundary layer becomes turbulent after the critical height has been reached.

Recommendations

The apparatus could be used to investigate the optimun pressure gradient and turbulence intensity of the main stream for heat transfer with grids or other turbulence promotors (see Shedden 29). The heat transfer studies could be done with or without frost deposition. It is also possible, with some small changes in the equipment, to do an investigation in which heat is transferred from a warm plate to the main stream.

Appendix

Nomenclature

c_p	in Lewis relation: average heat capacity of gas stream in coolant mass balance: average heat capacity of coolant in deposit energy balance: heat capacity of deposit
D	diffusion coefficient of water vapor through air
e	specific enthalpy
f_1	total heat transferred to plate surface without frosting
f_2	total heat transferred to frost surface when the frost surface temperature reaches the melting point. i.e. $T_s = T_{s,min}$
f_3	mass transfer rate at frost surface
h	height of deposit
h_{oo}	height of the deposit when the frost surface reaches the melting point.
H	non-dimensional thickness used by Libby and Chen. $H = h\, g_{c,o} / k_d\, T_p$
H_{oo}	free stream humidity
J	mass flux to the surface of the substrate
k	roughness height
k_{adm}	height beyond which the roughness affects the drag in the turbulent boundary layer
k_{air}	thermal conductivity of air
k_{ice}	thermal conductivity of ice
k_d	thermal conductivity of deposit
k_y	mass transfer coefficient
L'	non-dimensional latent heat of Libby and Chen $L' = (_d\, \rho_d / k_d)\ (L/T_s)$
L	heat of sublimation of species which deposits
l	length of brass plate

m mass flow rate of coolant to the plate

n constant which is a function of Re number and is used to calculate the intensity of turbulence in Eq.(50)

N_a internal diffusion mass flux caused by a temperature gradient across the deposit

Nu average Nusselt number. $Nu = h_{conv}\ l\ /\ k_{air}$

Pr Prandtl number. $Pr = \nu/\alpha$

$\bar{p}^2$ RMS value of the fluctuating component of power in the hot wire

P average power level of hot wire

P_o average power level of hot wire at zero velocity

P_s vapor pressure of deposit surface

q_{conv} heat transferred by convection to frost surface

q_{rad} heat transferred by radiation to frost surface

q_{mass} heat transferred to plate surface by solidification of vapor

q_w total heat flux through frost surface

$q_{w+\text{ heat leak}}$ total heat transferred to coolant without teflon plate on

$q_{T\text{ with tef}}$ total heat transferred with teflon plate on

$q_{\text{heat leak}}$ heat transferred to coolant not through frost deposit

Q non-dimensional heat transfer rate used by Libby and Chen. $Q = q_w\ h/\ k_d$

$q_{c,o}$ convective heat transfer to deposit surface with no deposition

R gas constant

Re Reynolds number. $Re = U_{oo}\ l\rho/\mu$

S volume fraction of frost deposit which is solid

T_{oo} static temperature of free stream

t	time
t_{min}	time to reach the quasi-steady state at which $T_s = T_{s,min}$
T_p	average temperature of brass plate surface
T_s	temperature of frost surface at air-frost interface
T'	dimensionless temperature. $T' = (T - T_p)/(T_{s,min} - T_p)$
$T_{s,min}$	melting point temprature of frost surface at air-frost interface
T_{out}	exit temperature of coolant from plate
T_{in}	inlet temperature of coolant to the plate
U_{∞}	free stream velocity
u	component of velocity in the x direction
v	component of velocity in the z direction
x	distance along the length of the plate surface
Y_{∞}	concentration in the free stream of the species which deposits
Y_s	concentration on the deposit surface of the species which deposits
z	coordinate normal to plate surface

Greek nomenclature

α	thermal diffusivity
α'	dimensionless thermal diffusivity . $\alpha' = \alpha_d \, t_{min}/h_{\infty}$
θ_1	dimensionless time. $\theta_1 = t/t_{min}$
ρ	density
η_1	dimensionless normal coordinate based on h_{∞}. $\eta_1 = z/h_{\infty}$
η	dimensionless normal coordinate based on h(t). $\eta = z/h$
η_h	dimensionless deposit height
$\bar{\eta}$	dimensionless coordinate of the Blasius laminar boundary layer solution $\bar{\eta} = z\sqrt{\frac{U_{\infty}}{\nu x}}$

Λ Schmidt number. Bird, Stewart, and lightfoot notation (Ref. 3) $\Lambda = \nu / D$

ν kinematic viscosity

ϕ parameter used by Bird, Stewart and Lightfoot, to calculate the effect of mass transfer on transfer coefficients

θ dimensionless temperature of Libby and Chen. $\theta = T_s/T_p$

$\bar{\theta}$ momentum thickness of boundary layer

π' dimensionless parameter used by Libby and Chen.

$$\pi' = (\alpha_d / k_d)\ (\pi / T_s)$$

π parameter to account for the effect of mass transfer on heat transfer. Suggested form of Libby and Chen:

$$\pi = \frac{\partial q_{conv}}{\partial\left[\frac{dh}{dt}\right]}$$

ΔH_s heat of sublimation of bulk crystals

ΔH_{des} activational free energy of desorption of deposited molecules upon brass plate

τ dimensionless time of Libby and Chen. $\tau = t q_{c,o}^2\ \alpha_d / k_d^2 T_p^2$

λ heat of vaporization of species which deposits

Subscripts

s property of frost deposit at frost surface

d property of deposit

g property of gas stream

L property of liquid phase

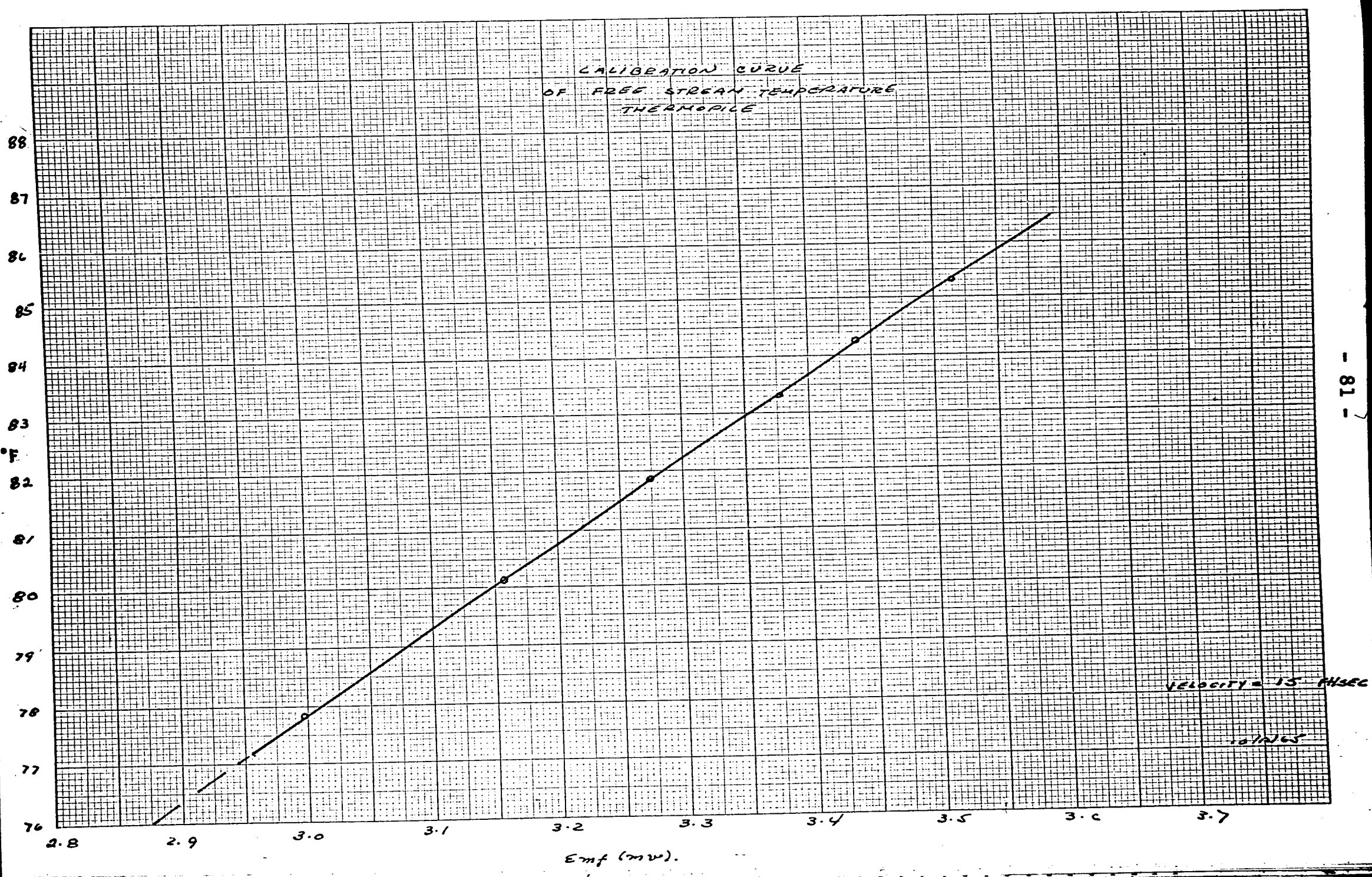
CALIBRATION CURVE
OF FREE STREAM TEMPERATURE
THERMOPILE
88
87
86
85
84
83
°F
82
81
80
79
78
77
76
2.8
2.9
3.0
3.1
3.2
3.3
3.4
3.5
3.6
3.7
Emf (mv).
VELOCITY = 15 FT/SEC
10 INCHES

CALIBRATION CURVE OF
WET BULB TEMPERATURE
THERMOPILE
90
85
80
75
70
65
60
T
F°
2.0
2.2
2.4
2.6
2.8
3.0
3.2
3.4
3.6
emf (mv)
VELOCITY = 1.5 FT/SEC
10 ft/sec

340 GABRIEL BIGURIA LAMINAR BOUNDARY LAYER VEL DISTR
MAY 20 66 21 19.2

```
#     SEQ  LABL TYP                    STATEMENT                                  C ZERO  NOT
001.           PL PROGRAM TO COMPUTE LAMINAR BOUNDARY LAYER                        [  ]  [
002.           PL VELOCITY DISTRIBUTIONS                                           [  ]  [
003.           PL GABRIEL BIGURIA     THESIS    340                                [  ]  [
004.           PL      H[IN]          V[FT/SEC]      V/V[1]    C                  [  ]  [
               .        ETA                                                       [  ]  [
005.           PV ,,                                                             [  ]  [
006.           CRDTAIR,   TOIL,  P     $TEMP IN DEG FAR.                         [  ]  [
007.           CRDHO,YO,Q,X  $ HO NULL PT,YOPROBE AT WALL                        [  ]  [
008.           D  H[100],V[100],Y[100],ETA[100]                                  [  ]  [
009.              I=0                                                            [  ]  [
010.      S10     I=I+1                                                          [  ]  [
011.           CRDH[I],Y[I]                                                      [  ]  [
012.              I=0                                                            [  ]  [
013.              I=0                                                            [  ]  [
014.      S20     I=I+1                                                          [  ]  [
015.              SPGO=0.9846-0.00042*[TOIL-50]                                  [  ]  [
016.              DAIR=0.0808*[[492/[460+TAIR]]*[P/760]]                         [  ]  [
017.              V[I]=[32.2*[H[I]-HO]*62.43*SPGO/[6*DAIR]]**  C                 [  ]  [
                  [1/2]                                                         [  ]  [
                  V[I]/V[1]                                                     [  ]  [
018.              NHU=[160+0.625*[TAIR-68]]*0.000001 $T DEG FAR                 [  ]  [
019.              ETA[I]=[[V[I]/[NHU*X*12]]**[1/2]]*[YO-Y[I]]                   [  ]  [
020.           PV H[I],V[I],V[I]/V[1],ETA[I]                                    [  ]  [
021.              I-0                                                           [  ]  [
022.           END$END OF PROGRAM
023.
```

*****SYMBOL TABLE*****

DAIR	ETA
H	I
P	Q
S20	SPGO
TOIL	V
YO	Y

UNUSED MEMORY FROM [OCTAL] 04745 TO [OCTAL] 16217.

340 GABRIEL BIGURIA LAMINAR BOUNDARY LAYER VEL DISTR
MAY 20 66 21 19.2 .


```
#     SEQ  LABL TYP   STATEMENT                                                  C ZERO  NOT 0  PLUS  MINUS  ELSE
001.            PL PROGRAM TO COMPUTE LAMINAR BOUNDARY LAYER                     [ ]     [ ]    [ ]   [ ]    [ ]
002.            PL VELOCITY DISTRIBUTIONS                                        [ ]     [ ]    [ ]   [ ]    [ ]
003.            PL GABRIEL BIGURIA     THESIS    340                             [ ]     [ ]    [ ]   [ ]    [ ]
004.            PL       H[IN]         V[FT/SEC]      V/V[1]      C
                          ETA
005.            PV ,,                                                            [ ]     [ ]    [ ]   [ ]    [ ]
006.            CRDTAIR,   TOIL,  P     $TEMP IN DEG FAR.                        [ ]     [ ]    [ ]   [ ]    [ ]
007.            CRDHO,YC,Q,X  $ HO NULL PT,YOPROBE AT WALL                       [ ]     [ ]    [ ]   [ ]    [ ]
008.            D  H[100],V[100],Y[100],ETA[100]                                 [ ]     [ ]    [ ]   [ ]    [ ]
009.               I=0                                                           [ ]     [ ]    [ ]   [ ]    [ ]
010.      S10      I=I+1                                                         [ ]     [ ]    [ ]   [ ]    [ ]
011.            CRDH[I],Y[I]                                                     [ ]     [ ]    [ ]   [ ]    [ ]
012.               I=0                                                           [ ]     [ ]    [ ]   [ ]    [ ]
013.               I=0                                                           [ ]     [ ]    [ ]   [S10 ]   [ ]
014.      S20      I=I+1                                                         [ ]     [ ]    [ ]   [ ]    [ ]
015.               SPGO=0.9846-0.00042*[TOIL-50]                                 [ ]     [ ]    [ ]   [ ]    [ ]
016.               DAIR=0.080A*[[492/[460+TAIR]]*[P/760]]                        [ ]     [ ]    [ ]   [ ]    [ ]
017.               V[I]=[32.2*[H[I]-HO]*62.43*SPGO/[6*DAIR]]**  C               [ ]     [ ]    [ ]   [ ]    [ ]
                   [1/2]
018.               V[I]/V[1]                                                     [ ]     [ ]    [ ]   [ ]    [ ]
019.               NHU=[160+0.625*[TAIR-68]]*0.000001 ST DEG FAR                 [ ]     [ ]    [ ]   [ ]    [ ]
020.               ETA[I]=[[V[I]/[NHU*X*12]]**[1/2]]*[YO-Y[I]]                   [ ]     [ ]    [ ]   [ ]    [ ]
021.            PV H[I],V[I],V[I]/V[1],ETA[I]                                    [ ]     [ ]    [ ]   [ ]    [ ]
022.               I=0                                                           [ ]     [ ]    [ ]   [ ]    [ ]
023.            END$END OF PROGRAM                                               [ ]     [ ]    [ ]   [S20 ]   [ ]
```

*****SYMBOL TABLE*****

DAIR	ETA	HO
H	I	NHU
P	Q	S10
S20	SPGO	TAIR
TOIL	V	X
YO	Y	

UNUSED MEMORY FROM [OCTAL] 04745 TO [OCTAL] 16217.

PAGE 1. MAY 20 66

0 PLUS MINUS ELSE

[S10]

[S20]

HO
NHU
S10
TAIR
X

PROGRAM TO COMPUTE LAMINAR BOUNDARY LAYER (with impact tube)
VELOCITY DISTRIBUTIONS
GABRIEL BIGURIA THESIS 340

H[IN]	V[FT/SEC]	V/V[1]	ETA
2.2090000-01	1.2607774+01	1.0000000+00	1.3808505+01
1.8790000-01	3.5833580+00	2.8421813-01	5.3194787-01
1.9050000-01	4.9348340+00	3.9141199-01	8.1558174-01
1.9250000-01	5.7626445+00	4.5707072-01	9.9522778-01
1.9450000-01	6.4856424+00	5.1441613-01	1.1729219+00
1.9900000-01	7.8732713+00	6.2447750-01	1.5319424+00
2.0400000-01	9.1720835+00	7.2749426-01	1.9629544+00
2.1110000-01	1.0750074+01	8.5265438-01	2.6563907+00
2.1460000-01	1.1448196+01	9.0802672-01	3.2055788+00
2.1800000-01	1.2087825+01	9.5875966-01	3.9207198+00
2.1890000-01	1.2251551+01	9.7174570-01	4.7008520+00

TYPE #END# STATEMENT EXECUTED.
CARDS REMAINING IN DECK ARE--

MAY 20 66 21 19.7

Hot - Wire Laminar Boundary Layer over Brass Plate

h_0 = 1.53 cm.

P [illegible]	h (cm)	V (ft/sec)	Eta	u/U_∞
1.475	2.04	11.6	6.86	0.966
1.45	1.81	10.8	3.63	0.900
1.39	1.72	9.00	2.56	0.750
1.31	1.65	6.91	1.62	0.576
1.21	1.60	4.76	0.94	0.396
1.12	1.58	3.10	0.54	0.258

PROGRAM TO COMPUTE LAMINAR BOUNDARY LAYER
VELOCITY DISTRIBUTIONS CASE OF BL TEFLON PLT
GABRIEL BIGURIA THESIS 340

H[IN]	V[FT/SEC]	V/V[1]	ETA
2.7650000-01	2.0067338+01	1.0000000+00	1.9509075+01
2.1250000-01	1.0987324+01	5.4752276-01	7.1784686-01
2.2100000-01	1.2576619+01	6.2672082-01	1.2904521+00
2.2750000-01	1.3667831+01	6.8109836-01	1.8346884+00
2.3540000-01	1.4886776+01	7.4184109-01	2.9860723+00
2.4580000-01	1.6353511+01	8.1493176-01	5.0157884+00
2.5600000-01	1.7674201+01	8.8074466-01	7.4491300+00
2.6350000-01	1.8585519+01	9.2615767-01	9.7928348+00
2.7320000-01	1.9701742+01	9.8178153-01	1.2339608+01
2.7380000-01	1.9768717+01	9.8511904-01	1.7869240+01
2.7500000-01	1.9901991+01	9.9176037-01	2.1185129+01

TYPE #END# STATEMENT EXECUTED.
MAY 20 66 21 19.1

Turbulent Boundary Layer Velocity Distribution over Teflon Plate. Data Shown in Fig. 8

$\bar{\theta}$ = Momentum Thickness = $\int_0^{\delta} \frac{u}{U_\infty} \left(1 - \frac{u}{U_\infty} \right) dy$

If the 7^{th} power law is assumed:

$$\bar{\theta} = 0.036 \times \left[\frac{U_\infty x}{\nu} \right]^{-1/5}$$

U_∞ = 20.06 ft/sec

$z/\bar{\theta}$	u/U_∞
0.785	0.548
1.32	0.628
1.80	0.681
2.28	0.742
2.81	0.815
4.50	0.881
6.44	0.926
8.25	0.982
10.2	0.985

Sample Calculation of Coolant Flow Rate

Assume:

The Brooks Turbine Flow Meter output reads: 11.0%
Temperature of Fluid (Freon 11); 40°F
Viscosity of Freon 11 at 40°F: 0.85 cp or 0.508 CTKS
Density of Freon 11 at 40°F : 1.525 g/cc or 95.1 lb_m/ft^3

$$\text{Flow rate } (lb_m/hr) = \frac{(\text{Frequency -CPS-}) \times 3600 \times \text{Sp.Gr.} \times 8.34}{\text{Cycles per gallon}}$$

From the Brooks calibration chart at a reading of 11.0%:

the frequency is = 56.7 cps
k= the cycles/gallon = 6173

Now, to correct k (cycles / gallon) for the effect of viscosity since chart was calibrated for water viscosity:

$$\nu_{calibration} = \frac{0.84}{0.996} = 0.844 \quad (\text{up to } 20\%)$$

$$cps/\nu_{water} = \frac{56.7}{0.884} = 67.3 \quad \text{gives from chart } k = 6990$$

$$cps/\nu_{Freon} = \frac{56.7}{0.508} = 111.8 \quad \text{gives from chart } k = 7025$$

Hence, the correction in k due to the difference in viscosity between Freon 11 and water is: 7025 - 6990 = 35

Therefore, at 11.0 %:

$$k_{Freon} = 6173 + 35 = 6208 \text{ cycles/gallon}$$

$$\text{flow rate} = \frac{56.7 \times 3600 \times 95.1 \times 8.345}{6208 \times 62.43}$$

$$= 418.0 lb_m / hr$$

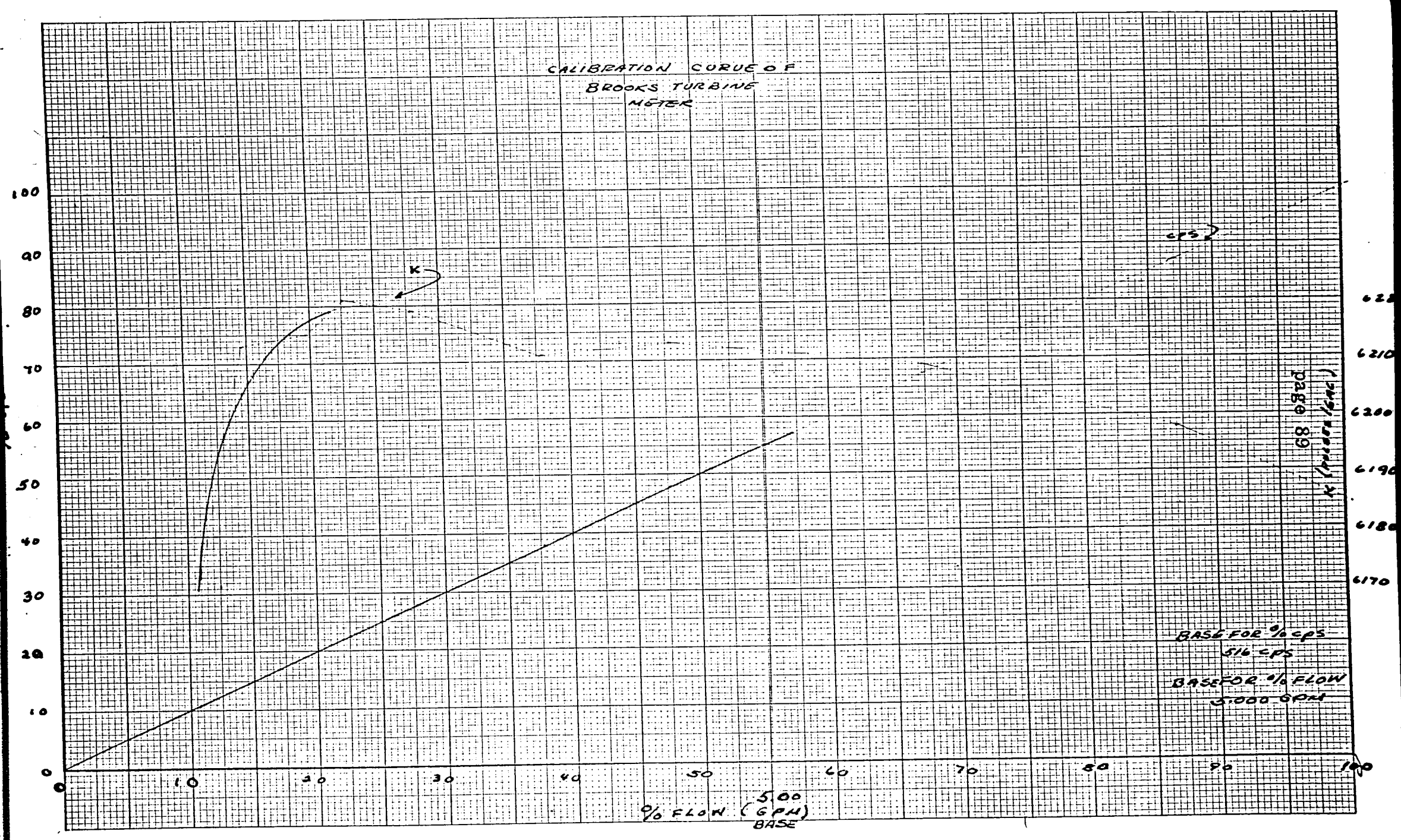
CALIBRATION CURVE OF
BROOKS TURBINE
METER
100
90
80
70
60
50
40
30
20
10
0
K
CPS
6220
6210
6200
6190
6180
6170
page 89
BASE FOR 0% CPS
516 CPS
BASE FOR 0% FLOW
5.000 GPM
10
20
30
40
50
60
70
80
90
100
0
5.00
% FLOW (GPM)
BASE

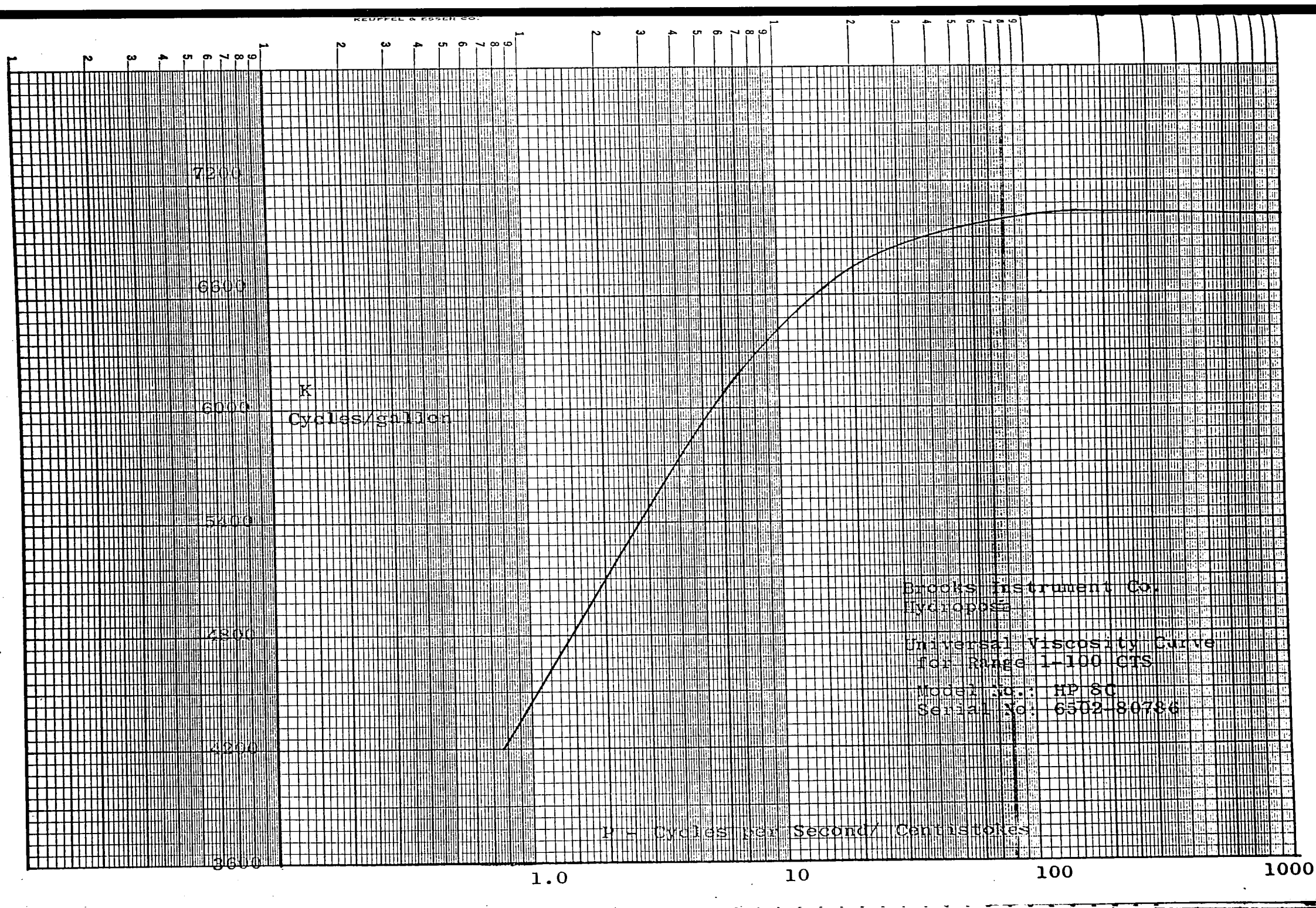
KEUFFEL & ESSER CO.
7200
6600
6000
5400
4800
4200
3600
K
Cycles/Gallon
1.0
10
100
1000
p - Cycles per Second/ Centistokes
Brooks Instrument Co.
Hatfield, Pa.
Universal Viscosity Curve
for Range 1-100 CTS
Model No.: HP 8C
Serial No.: 6502-80786

Sample Calculation of Experimental Nusselt Numbers

assume pt. 1. : Teflon plate over brass plate

T_{∞} = 78.8°F ,
U_{oo} = 18.16 ft/sec
$\Delta T_{coolant}$ = 1.101 °F
m (%) = 11.2 %
m (lb /hr) = 429

$m\ c_p\ \Delta T_{coolant}$ = 95.9 Btu/hr

$T_{Teflon\ surface}$ = 70°F

From computer program :

$q_{rad.\ to\ teflon\ surface}$ = 4.24 Btu/ hr

$q_{conv.\ turbulent\ to\ teflon\ surface}$ = 33.24

sum 37.48 Btu/hr

Hence, heat leaks is:

95.9 Btu/hr
- 37.5
heat leak 58.4 Btu/hr

Now, pt. 1, no teflon plate over brass plate:

T_{oo} = 79.0°F Area Plate = 0.626 ft^2
T_p = 43.6 °F length Plate= 0.92167
k_{air} = 0.0146 Btu/ hr ft °F
U_{oo} = 17.88 ft/sec m = 11.2 % = 429 lb/hr
$\Delta T_{coolant}$ = 1.1462 F°
$\Delta T_{boundary\ layer}$ = $(T_{\infty} - T_p)$ = 35.4F°

Total non-corrected heat flux is: $m\ c_p\ \Delta T$ = 127.2 Btu/hr

Total corrected heat flux is: 127.2 - 58.4 =68.8 Btu/hr

$$Nu = \frac{q_{corrected} \times length}{\Delta T_{b.l.}\ Area \times k_{air}} = \frac{68.8 \times 0.92167}{35.4 \times 0.626 \times 0.0146} = 196$$

340 GABRIEL BIGURIA PROGRAM TO COMPUTE HEAT TRANSFER COEFFICIENTS
MAY 21 66 11 43.9

```
#     SEQ  LABL TYP                    STATEMENT                          C ZERO    NOT
001.           PL PROGRAM TO COMPUTE  HEAT TRANSFER COEFFICIENTC
                  S AND CONVECTIVE AND RADIATIVE HEAT FLUXES TOC
                  TEFLON PLATE                                            [    ]  [
002.           PL GABRIEL BIGURIA   THESIS   340                          [    ]  [
003.           PL       V[I]          RET[I]              REP[I]C
                          HCT[I]          QCL[I]          QCTC
                           QR1             QR2                            [    ]  [
004.           PV ,,                                                     [    ]  [
005.           CRDPR,C,L  $Q=NP OF POINTS,L=LENGHT IN FT                 [    ]  [
006.           D  TAIR[50],TP[50],TT[50],V[50],RET[50],HCL[50],C
                  QCL[50],QCT[50],KAIRT[50],NHUT[50],QR1[53]              [    ]  [
007.           D  QR2[50],HCT[50],TFT[50],TFP[50],KAIRP[50]               [    ]  [
008.           D  NHUP[50],REP[50]                                        [    ]  [
009.              I=0                                                     [    ]  [
010.       S10    I=I+1                                                   [    ]  [
011.           CRDV[I],TAIR[I],TP[I],TT[I]                               [    ]  [
012.              I-Q                                                     [    ]  [
013.              I=0                                                     [    ]  [
014.       S20    I=I+1                                                   [    ]  [
015.              TFP[I]=[TP[I]+TAIR[I]]/2                                [    ]  [
016.              TFT[I]=[TT[I]+TAIR[I]]/2                                [    ]  [
017.              KAIRP[I]=0.0140+0.0000206*[TFP[I]-32]                   [    ]  [
018.              KAIRT[I]=0.0140+0.0000206*[TFT[I]-32]                   [    ]  [
019.              NHUT[I]=[160+0.565*[TFT[I]-68]]*0.000001                [    ]  [
020.              NHUP[I]=[160+0.565*[TFP[I]-68]]*0.000001                [    ]  [
021.              RET[I]=[V[I]*L]/NHUT[I]                                 [    ]  [
022.              REP[I]=[V[I]*L]/NHUP[I]                                 [    ]  [
023.              HCT[I]=[0.036*[PR**0.333]*[RET[I]**0.8]*KAIRTC
                  [I]]/L                                                  [    ]  [
024.              HCL[I]=0.664*[PR**0.333]*[REP[I]**0.5]*KAIRP C
                  [I]/L                                                   [    ]  [
025.              QCL[I]=HCL[I]*0.6262*[TAIR[I]-TP[I]]                    [    ]  [
026.              QCT[I]=HCT[I]*0.6262*[TAIR[I]-TT[I]]                    [    ]  [
027.              QR1[I]=0.171*0.6262*0.81*[0.21*[[[TAIR[I]+460C
                  C
                  ]/100 ]                                                 [    ]  [
                  **4]-0.21*[[[TP[I]+460]/100]**4]]
                   QR2[I]=0.171*0.6262*0.81*[0.91*[[[TAIR[I]+46C
028.              C
                  0]/100                                                  [    ]  [
                  ]**4]-0.91*[[[TT[I]+460]/100]**4]]
029.       PV V[I],RET[I],REP[I],HCT[I],QCL[I],QCT[I],          C
                  QR1[I],QR2[I]                                           [    ]  [
030.              I-0                                                     [    ]  [
031.           END $END OF PROGRAM                                        [    ]  [
```

```
    340  GABRIEL BIGURIA  PROGRAM TO COMPUTE HEAT TRANSFER COEFFICIENTS
MAY 21 66       11 43.9
                                                                           PAGE 1.      MAY 21 66

  #      SEQ  LABL TYP                 STATEMENT                  C ZERO    NOT 0     PLUS     MINUS     ELSE

001.                PL PROGRAM TO COMPUTE  HEAT TRANSFER COEFFICIENTC
  .                    S AND CONVECTIVE AND RADIATIVE HEAT FLUXES TOC
  .                    TEFLON PLATE                               [    ]   [    ]   [    ]   [    ]   [    ]
002.                PL GABRIEL BIGURIA   THESIS   340             [    ]   [    ]   [    ]   [    ]   [    ]
003.                PL          V[I]             RET[I]         REP[I]C
  .                          HCT[I]           QCL[I]          QCTC
  .                           QR1              QR2                [    ]   [    ]   [    ]   [    ]   [    ]
004.                PV ,,                                         [    ]   [    ]   [    ]   [    ]   [    ]
005.                CRDPR,C,L  $Q=NP OF POINTS,L=LENGHT IN FT     [    ]   [    ]   [    ]   [    ]   [    ]
006.                D  TAIR[50],TP[50],TT[50],V[50],RET[50],HCL[50],C
  .                    QCL[50],QCT[50],KAIRT[50],NHUT[50],QR1[53] [    ]   [    ]   [    ]   [    ]   [    ]
007.                D  QR2[50],HCT[50],TFT[50],TFP[50],KAIRP[50]  [    ]   [    ]   [    ]   [    ]   [    ]
008.                D  NFUP[50],REP[50]                           [    ]   [    ]   [    ]   [    ]   [    ]
009.                   I=0                                        [    ]   [    ]   [    ]   [    ]   [    ]
010.           S10     I=I+1                                      [    ]   [    ]   [    ]   [    ]   [    ]
011.                CRDV[I],TAIR[I],TP[I],TT[I]                   [    ]   [    ]   [    ]   [    ]   [    ]
012.                   I-Q                                        [    ]   [    ]   [    ]   [S10 ]   [    ]
013.                   I=0                                        [    ]   [    ]   [    ]   [    ]   [    ]
014.           S20     I=I+1                                      [    ]   [    ]   [    ]   [    ]   [    ]
015.                   TFP[I]=[TP[I]+TAIR[I]]/2                   [    ]   [    ]   [    ]   [    ]   [    ]
016.                   TFT[I]=[TT[I]+TAIR[I]]/2                   [    ]   [    ]   [    ]   [    ]   [    ]
017.                   KAIRP[I]=0.0140+0.0000206*[TFP[I]-32]      [    ]   [    ]   [    ]   [    ]   [    ]
018.                   KAIRT[I]=0.0140+0.0000206*[TFT[I]-32]      [    ]   [    ]   [    ]   [    ]   [    ]
019.                   NHUT[I]=[160+0.565*[TFT[I]-68]]*0.000001   [    ]   [    ]   [    ]   [    ]   [    ]
020.                   NFUP[I]=[160+0.565*[TFP[I]-68]]*0.000001   [    ]   [    ]   [    ]   [    ]   [    ]
021.                   RET[I]=[V[I]*L]/NHUT[I]                    [    ]   [    ]   [    ]   [    ]   [    ]
022.                   REP[I]=[V[I]*L]/NFUP[I]                    [    ]   [    ]   [    ]   [    ]   [    ]
023.                   HCT[I]=[0.036*[PR**0.333]*[RET[I]**0.8]*KAIRTC
  .                    [I]]/L                                     [    ]   [    ]   [    ]   [    ]   [    ]
024.                   HCL[I]=0.664*[PR**0.333]*[REP[I]**0.5]*KAIRP C
  .                    [I]/L                                      [    ]   [    ]   [    ]   [    ]   [    ]
025.                   QCL[I]=HCL[I]*0.6262*[TAIR[I]-TP[I]]       [    ]   [    ]   [    ]   [    ]   [    ]
026.                   QCT[I]=HCT[I]*0.6262*[TAIR[I]-TT[I]]       [    ]   [    ]   [    ]   [    ]   [    ]
027.                   QR1[I]=0.171*0.6262*0.81*[0.21*[[[TAIR[I]+460C
  .                    ]/100 ]                                   C
  .                    **4]-0.21*[[[TP[I]+460]/100]**4]]          [    ]   [    ]   [    ]   [    ]   [    ]
028.                   QR2[I]=0.171*0.6262*0.81*[0.91*[[[TAIR[I]+46C
  .                    0]/100                                    C
  .                    ]**4]-0.91*[[[TT[I]+460]/100]**4]]         [    ]   [    ]   [    ]   [    ]   [    ]
029.     /          PV V[I],RET[I],REP[I],HCT[I],QCL[I],QCT[I],      C
  .                    QR1[I],QR2[I]                              [    ]   [    ]   [    ]   [    ]   [    ]
030.                   I-Q                                        [    ]   [    ]   [    ]   [S20 ]   [    ]
031.                END $END OF PROGRAM                           [    ]   [    ]   [    ]   [    ]   [    ]
```

```
ADIATIVE HEA
   QCL[I]

)000+00   2.
)162+01   0.
)000+00   3.
)422+01   0.
0000+00   3.
9273+01   0.
0000+00   2.
4039+01   0.
0000+00   4.
4912+01   0.
0000+00   3.
7201+01   0.
0000+00   3.
0473+01   0.
0000+00   3.
0542+01   0.
0000+00   3.
4646+01   0.
0000+00   3.
3142+01   0.
0000+00   4.
8392+01   0.
0000+00   4.
5819+02   0.
```

PROGRAM TO COMPUTE HEAT TRANSFER COEFFICIENTS AND CONVECTIVE AND RADIATIVE HEAT FLUXES TOTEFLON PLATE
GABRIEL BIGURIA THESIS 340

V[I]	RMT[I]	REP[I]	HCT[I]	QCL[I]	QCT	QR1	QR2
1.8160000+01	1.0229762+05	1.0076656+05	5.3030121+00	0.0000000+00	2.9222566+01	0.0000000+00	4.2404023+00
1.7880000+01	9.9145442+04	1.0549251+05	5.2048300+00	6.7900162+01	0.0000000+00	3.6579708+00	0.0000000+00
2.1640000+01	1.2160695+05	1.1991330+05	6.0956183+00	0.0000000+00	3.1300025+01	0.0000000+00	3.9667957+00
2.1400000+01	1.1858339+05	1.2582827+05	6.0079588+00	7.1109422+01	0.0000000+00	3.5218084+00	0.0000000+00
2.5720000+01	1.4423657+05	1.4242496+05	6.9931325+00	0.0000000+00	3.2405337+01	0.0000000+00	3.5918068+00
2.5280000+01	1.3989347+05	1.4824124+05	6.8609582+00	7.5669273+01	0.0000000+00	3.4638085+00	0.0000000+00
1.2810000+01	7.2599104+04	7.1201473+04	4.0208816+00	0.0000000+00	2.8452000+01	0.0000000+00	5.3919853+00
1.2810000+01	7.1274330+04	7.5036577+04	3.9915056+00	4.7694039+01	0.0000000+00	3.0719600+00	0.0000000+00
2.3460000+01	1.3219885+05	1.2982203+05	6.5095682+00	0.0000000+00	4.3208691+01	0.0000000+00	5.1050464+00
2.2980000+01	1.2729537+05	1.3550914+05	6.3594228+00	7.7624912+01	0.0000000+00	3.6922259+00	0.0000000+00
2.4980000+01	1.4083714+05	1.3884565+05	6.8462625+00	0.0000000+00	3.5583175+01	0.0000000+00	3.9938300+00
2.4460000+01	1.3586276+05	1.4454996+05	6.6922127+00	7.9207201+01	0.0000000+00	3.6381832+00	0.0000000+00
4.2860000+01	2.4006804+05	2.3798430+05	1.0516931+01	0.0000000+00	3.3587081+01	0.0000000+00	2.4802271+00
4.1590000+01	2.3061851+05	2.4102349+05	1.0225950+01	7.4160473+01	0.0000000+00	2.6993555+00	0.0000000+00
4.4600000+01	2.4955709+05	2.4739319+05	1.0852692+01	0.0000000+00	3.4659374+01	0.0000000+00	2.4843941+00
4.3700000+01	2.4240095+05	2.5329641+05	1.0640353+01	7.5720542+01	0.0000000+00	2.6879499+00	0.0000000+00
2.2670000+01	1.2743899+05	1.2570622+05	6.3275093+00	0.0000000+00	3.1698291+01	0.0000000+00	3.8678639+00
2.2420000+01	1.2457403+05	1.3295185+05	6.2426873+00	7.9514646+01	0.0000000+00	3.7930114+00	0.0000000+00
3.0080000+01	1.6868725+05	1.6656854+05	7.9264229+00	0.0000000+00	3.6730092+01	0.0000000+00	3.5918068+00
2.9780000+01	1.6513150+05	1.7662916+05	7.8280264+00	9.4863142+01	0.0000000+00	3.9255027+00	0.0000000+00
3.5120000+01	1.9701907+05	1.9460975+05	8.9734202+00	0.0000000+00	4.0457922+01	0.0000000+00	3.4927658+00
3.4660000+01	1.9173511+05	2.0405218+05	8.8301452+00	9.5048392+01	0.0000000+00	3.6913924+00	0.0000000+00
4.0970000+01	2.2928493+05	2.2671818+05	1.0140794+01	0.0000000+00	4.1911089+01	0.0000000+00	3.2142477+00
3.9900000+01	2.2064736+05	2.3639438+05	9.8815532+00	1.1265819+02	0.0000000+00	4.0352563+00	0.0000000+00

TYPE #END# STATEMENT EXECUTED.
CARDS REMAINING IN DECK ARE--

MAY 21 66 11 44.5

a)

s plate

s) nd Re Numbers

$mc_p\Delta T$	Nu	Re
5.9 7.2	196	1.05 x10^5
0.2 7.5	229	1.25 x10^5
2.0 9	234	1.48 x10^5
3.8 4.5	166	7.50 x10^4
05.7 13	224	1.36 x10^5
01 12	246	1.44 x10^5
7.0 1	465	2.41 x10^5
7 1.8	495	2.53 x10^5
3 8	204	1.33 x10^5
3 9.6	267	1.77 x10^5
1 3	344	2.04 x10^5
05 12	416	2.36 x10^5

T FLUXEB TOTEFLON PLATE

	QCT	QR1	QR2
9222566+01	0.0000000+00	4.2404023+00	
0000000+00	3.6579708+00	0.0000000+00	
1300025+01	0.0000000+00	3.9667957+00	
0000000+00	3.5218084+00	0.0000000+00	
2405337+01	0.0000000+00	3.5918068+00	
0000000+00	3.4638085+00	0.0000000+00	
8452000+01	0.0000000+00	5.3919853+00	
0000000+00	3.0719600+00	0.0000000+00	
3208691+01	0.0000000+00	5.1050464+00	
0000000+00	3.6922259+00	0.0000000+00	
5583175+01	0.0000000+00	3.9938300+00	
0000000+00	3.6381832+00	0.0000000+00	
3587081+01	0.0000000+00	2.4802271+00	
0000000+00	2.6993555+00	0.0000000+00	
4659374+01	0.0000000+00	2.4843941+00	
0000000+00	2.6879499+00	0.0000000+00	
1698291+01	0.0000000+00	3.8678639+00	
0000000+00	3.7930114+00	0.0000000+00	
6730092+01	0.0000000+00	3.5918068+00	
0000000+00	3.9255027+00	0.0000000+00	
0457922+01	0.0000000+00	3.4927658+00	
0000000+00	3.6913924+00	0.0000000+00	
1911089+01	0.0000000+00	3.2142477+00	
0000000+00	4.0352563+00	0.0000000+00	

Reduced Heat Transfer Data
to Teflon Plate and Brass plate
Experimental Nu Numbers and Re Numbers

pt.	T_∞	T_p	U_∞	T_{Ts}	$\Delta T_{cool.}$	m(%)	$\dot{m}$(lb/hr)	$mc_p\Delta T$	Nu	Re
1	78.8	42.7	1816	70	1.101	11.2	429	95.9		
1	79.0	43.6	17.88	-	1.462	11.2	429	127.2	196	1.05 x10^5
2	79.2	44.6	21.64	71	1.039	11.2	428	90.2		
2	79.2	45.3	21.40	-	1.469	11.2	428	127.5	229	1.25 x10^5
3	79.4	45.2	25.72	72	1.004	11.7	446	92.0		
3	79.6	46.4	25.28	-	1.40	11.9	454	129	234	1.48 x10^5
4	78.3	47.5	12.81	67	0.854	11.2	426	73.8		
4	78.0	48.6	12.81	-	0.968	13.3	430	84.5	166	7.50 x10^4
5	79.6	43.2	23.46	69	1.082	11.4	436	95.7		
5	79.3	43.6	22.98	-	1.53	11.2	428	133	224	1.36 x10^5
6	78.3	43.2	24.98	70	1.181		421	101		
6	78.5	43.2	24.46	-	1.66		421	142	246	1.44 x10^5
7	78.6	55.0	42.86	73	0.994		417	87.0		
7	79.0	53.6	41.59	-	1.875		417	164	465	2.41 x10^5
8	78.9	54.6	44.60	74	0.994		417	87		
8	78.9	53.6	43.70	-	1.96		417	171.8	495	2.53 x10^5
9	79.0	40.9	22.67	71	1.31	11.0	422	113		
9	78.4	41.4	22.42	-	1.71	11.0	422	148	204	1.33 x10^5
10	79.4	39.8	30.08	72	1.538	11.0	422	133		
10	79.0	40.7	29.78	-	2.17	11.0	422	189.6	267	1.77 x10^5
11	79.2	42.0	35.12	72	1.36	11.0	421	121		
11	79.7	44.1	34.66	-	2.24	10.9	416	193	344	2.04 x10^5
12	79.6	38.0	40.97	73	1.562	11.0	423	135		
12	79.8	40.5	39.9	-	2.855	11.0	422	252	416	2.36 x10^5

Sample Calculation of Frost Thermal Conductivity

Run Conditions :

R.H. 26 %
T_p = - 20°F
T_∞ = 79 °F
U_{oo} = 21.6 ft/sec

Calculation of Heat Leak: Teflon plate on

mass flow rate: indicator reading = 11.0%
T_{Freon} = -24°F
mass flow rate = 444 lb_m/hr

Total heat with teflon plate on = $mc_p \Delta T_{coolant}$
= 444 x 0.196 x 3.50
= 304 Btu/hr

from computer program:

$q_{rad\ to\ Teflon\ plate}$ = 8.46 Btu/hr
$q_{conv.\ to\ teflon\ plate}$ = 68.62
77.08 Btu/hr

hence heat leak = 304 - 77.1 = 227 Btu / hr

Calculation of Frost Thermal Conductivity:

A point in time for this run, shows that at 22.5 minutes from the beginning of deposition, the total heat flux is:

q_{total} = 421 Btu/hr

and the corrected heat flux is:

q_w = 421 - 227 = 194 Btu/hr or 310 Btu/hr ft^2

From the data shown in Figures 16 and 17:

T_{Fs} = 1.5°F h = 0.0430 inches

Hence, $k_{frost} = \frac{q_w \times h}{\Delta T_{frost}} = \frac{310 \times 0.0430}{12 \times 21.5} = 0.0516 \frac{Btu}{hr\ ft\ °F}$

Frost Thermal Conductivity Data

Run: R.H. = 26 % T_p = - 20°F
U_{oo} = 21.6 ft/sec

Time (min)	q_w (Btu/hr ft^2)	T_{Fs} (°F)	$T_{avg.f}$	h(in)	k_{frost} (Btu/hr ft °F)
8	363	-5	-12.5	0.030	0.0605
14	318	-1.5	-10.8	0.036	0.0516
22.5	310	+1.5	- 9.2	0.043	0.0516
36.5	300	5.0	- 7.5	0.048	0.0480
50	294	7.0	- 7.0	0.056	0.0517
63	292	9.5	-5.2	0.070	0.0576

Run: R.H. = 46 % T_p = - 18°F
U_∞ = 21.6 ft/sec

Time	q_w	T_{Fs}	$T_{avg.}$	h	k_{frost}
3.5	385	4.5	-6.75	0.0312	0.0449
12.5	342	17.5	-0.25	0.059	0.0474
19	411	22	+2.0	0.1142	0.0978
45	576	28	5.0	0.1175	0.1227
58	584	28	5.0	0.1575	0.1669
62	542	28	5.0	0.1611	0.1585
70	542	27	4.5	0.1575	0.1581

Run: R.H.= 70 % T_p = - 19°F
U_∞ = 21.6 ft/sec

Time	q_w	T_{Fs}	$T_{avg.}$	h	k_{frost}
2.25	482	7.5	-5.75	0.016	0.0237
5	460	17.5	-0.75	0.031	0.0328
12.5	393	28	+4.5	0.051	0.0356
22.5	610	28	4.5	0.126	0.1361
47	708	30	5.5	0.1255	0.1510

Sample Calculation of Heat Flux Prediction from Lewis Relation

Lewis Relation: $\frac{h_{conv}}{c_p} = k_y = KGL$ (in computer notation)

hence,

$$q_w = q_{mass} + q_{conv} + q_{rad} = h\left[(T_\infty - T_s) + \frac{L}{c_p} (P_\infty - P_s)\right] + q_{rad}$$

$$q_{mass} = KGL \times L \times (P_\infty - P_s) = \frac{KGL \times 1210 \times 18}{760} (P_\infty - P_s)$$

for a stream at 80°F and

$U_\infty = 21.6$ ft/sec

R.H. = 70 % or H = 0.0161 $lb_{H_2O}/lb_{dry\ air}$

$$P_\infty = \frac{H\,P}{0.622 + H} = \frac{0.0161 \times 760}{0.622 + 0.016}$$

P_{oo} = 19.18 m m Hg

When T_{Fs} = - 20 °F

P_s = 0.30 mm Hg (From Perry' s Fourth Ed.)

$P_{oo} - P_s$ = 18.88

From computer program and Lewis Relation: KGL = 0.491

$$q_{mass} = 1210 \times 18 \times \frac{(0.491)}{760} \times 18.88 = 166 \text{ Btu/hr}$$

Also from computer program:

QCL = q_{conv}	=	214
QRl = q_{rad}	=	40
		250 Btu/hr

Therefore, total heat flux to frost surface:

q_w = 250 + 166 = 416 Btu/ hr or 664 Btuphr ft^2

340 GABRIEL BIGURIA PROGRAM TO COMPUTE HEAT AND MASS TRANSFER COEFF
MAY 20 66 21 20:43


```
#     SEQ  LABL TYP  STATEMENT                                  C ZERO  NOT 0  PLUS  MINUS  ELSE
001.            PL  PROGRAM TO COMPUTE HEAT AND MASS TRANSFER  C
.                   COEFFICIENTS FROM LEWIS RELATION            [ ]     [ ]    [ ]   [ ]    [ ]
002.            PL  GABRIEL BIGURIA  THESIS  340               [ ]     [ ]    [ ]   [ ]    [ ]
003.            CRDPR,Q,L  SQ=NP OF POINTS,L=LENGHT IN FT      [ ]     [ ]    [ ]   [ ]    [ ]
004.            D   TAIR[50],TP[50],TT[50],V[50],RET[50],HCL[50],C
.                   QCL[50],QCT[50],KAIRT[50],NHUT[50],QR1[53]  [ ]     [ ]    [ ]   [ ]    [ ]
005.            D   QR2[50],HCT[50],TFT[50],TFP[50],KAIRP[50]   [ ]     [ ]    [ ]   [ ]    [ ]
006.            D   NHUP[50],REP[50]                           [ ]     [ ]    [ ]   [ ]    [ ]
007.            D   DAIRL[50],DAIRT[50],KGL[50],KGT[50]        [ ]     [ ]    [ ]   [ ]    [ ]
008.                I=0                                        [ ]     [ ]    [ ]   [ ]    [ ]
009.        S10     I=I+1                                      [ ]     [ ]    [ ]   [ ]    [ ]
010.            CRDV[I],TAIR[I],TP[I],TT[I]                    [ ]     [ ]    [ ]   [ ]    [ ]
011.                I-Q                                        [ ]     [ ]    [ ]   [S10 ] [ ]
012.                I=0                                        [ ]     [ ]    [ ]   [ ]    [ ]
013.        S20     I=I+1                                      [ ]     [ ]    [ ]   [ ]    [ ]
014.                TFP[I]=[TP[I]+TAIR[I]]/2                   [ ]     [ ]    [ ]   [ ]    [ ]
015.                TFT[I]=[TT[I]+TAIR[I]]/2                   [ ]     [ ]    [ ]   [ ]    [ ]
016.                KAIRP[I]=0.0140+0.0000206*[TFP[I]-32]      [ ]     [ ]    [ ]   [ ]    [ ]
017.                KAIRT[I]=0.0140+0.0000206*[TFT[I]-32]      [ ]     [ ]    [ ]   [ ]    [ ]
018.                NHUT[I]=[160+0.565*[TFT[I]-68]]*0.000001   [ ]     [ ]    [ ]   [ ]    [ ]
019.                NHUP[I]=[160+0.565*[TFP[I]-68]]*0.000001   [ ]     [ ]    [ ]   [ ]    [ ]
020.                DAIRT[I]=0.0808*[492/[460+TFT[I]]]         [ ]     [ ]    [ ]   [ ]    [ ]
021.                DAIRL[I]=0.0808*[492/[460+TFP[I]]]         [ ]     [ ]    [ ]   [ ]    [ ]
022.                REP[I]=[V[I]*L]/NHUP[I]                    [ ]     [ ]    [ ]   [ ]    [ ]
023.                RET[I]=[V[I]*L]/NHUT[I]                    [ ]     [ ]    [ ]   [ ]    [ ]
024.                HCT[I]=[0.036*[PR**0.333]*[RET[I]**0.8]*KAIRTC
.                   [I]]/L                                     [ ]     [ ]    [ ]   [ ]    [ ]
025.                HCL[I]=0.664*[PR**0.333]*[REP[I]**0.5]*KAIRP C
.                   [I]/L                                      [ ]     [ ]    [ ]   [ ]    [ ]
026.                QCL[I]=HCL[I]*0.6262*[TAIR[I]-TP[I]]       [ ]     [ ]    [ ]   [ ]    [ ]
027.                QCT[I]=HCT[I]*0.6262*[TAIR[I]-TT[I]]       [ ]     [ ]    [ ]   [ ]    [ ]
028.                QR1[I]=0.171*0.6262*0.81*[0.97*[[[TAIR[I]+460C
.                   ]/100 ]                                    C
.                   **4]-0.97*[[[TP[I]+460]/100]**4]]          [ ]     [ ]    [ ]   [ ]    [ ]
029.                 QR2[I]=0.171*0.6262*0.81*[0.91*[[[TAIR[I]+46C
.                   0]/100                                     C
.                   ]**4]-0.91*[[[TT[I]+460]/100]**4]]         [ ]     [ ]    [ ]   [ ]    [ ]
030.                KGL[I]=HCL[I]/[DAIRL[I]*0.240*0.730*[TFP[I]+ C
.                   460]]                                      [ ]     [ ]    [ ]   [ ]    [ ]
031.                KGT[I]=HCT[I]/[DAIRT[I]*0.240*0.730*[TFT[I]+ C
.                   460]]                                      [ ]     [ ]    [ ]   [ ]    [ ]
032.                I-Q                                        [ ]     [ ]    [ ]   [S20 ] [ ]
033.            PL      V[I]          RET[I]          REP[I]C
.                         HCT[I]          QCL[I]          QCTC
.                          QR1             QR2               [ ]     [ ]    [ ]   [ ]    [ ]
034.            PV  ,,                                         [ ]     [ ]    [ ]   [ ]    [ ]
035.                I=0                                        [ ]     [ ]    [ ]   [ ]    [ ]
036.        S30     I=I+1                                      [ ]     [ ]    [ ]   [ ]    [ ]
037.            PV  V[I],RET[I],REP[I],HCT[I],QCL[I],QCT[I],   C
.                   QR1[I],QR2[I]                              [ ]     [ ]    [ ]   [ ]    [ ]
038.                I-Q                                        [ ]     [ ]    [ ]   [S30 ] [ ]
039.            PV  ,,                                         [ ]     [ ]    [ ]   [ ]    [ ]
040.            PL          TT              KGL             KGT [ ]     [ ]    [ ]   [ ]    [ ]
041.                I=0                                        [ ]     [ ]    [ ]   [ ]    [ ]
042.        S40     I=I+1                                      [ ]     [ ]    [ ]   [ ]    [ ]
```

#	SEQ	LABL	TYP	STATEMENT	C ZERO	NOT 0	PLUS	MINUS	ELSE
043.				PV TT[I],KGL[I],KGT[I]	[ ]	[ ]	[ ]	[ ]	[ ]
044.				I-Q	[ ]	[ ]	[ ]	[S40]	[ ]
045.				END $END OF PROGRAM	[ ]	[ ]	[ ]	[ ]	[ ]

*****SYMBOL TABLE*****

DAIRL	DAIRT	HCL
HCT	I	KAIRT
KAIRP	KGI	KGT
L	NHIIT	NHUP
PR	Q	QCL
QCT	QR1	QR2
RET	REP	S10
S20	S30	S40
TAIR	TP	TT
TFT	TFP	V

UNUSED MEMORY FROM [OCTAL] 05412 TO [OCTAL] 13343.

PROGRAM TO COMPUTE HEAT AND MASS TRANSFER COEFFICIENTS FROM LEWIS RELATION
GABRIEL BIGURIA THESIS 340

V[I]	RET[I]	REP[I]	HCT[I]	QCL[I]	QCT	QR1	QR2
2.1600000+01	1.2314265+05	1.1940771+05	6.1217672+00	0.0000000+00	6.8618766+01	0.0000000+00	8.4612173+00
2.1600000+01	1.2173864+05	1.1956980+05	6.0937230+00	0.0000000+00	4.0066838+01	0.0000000+00	5.0554572+00
2.1600000+01	1.2199153+05	1.1884387+05	6.0987743+00	0.0000000+00	5.8431502+01	0.0000000+00	7.3425307+00
2.1600000+01	1.2059286+05	1.1777137+05	6.0708369+00	0.0000000+00	5.3221813+01	0.0000000+00	6.8457387+00
2.1600000+01	1.1936726+05	1.4370946+05	6.0463573+00	2.1398739+02	0.0000000+00	4.0004857+01	0.0000000+00
2.1600000+01	1.1936726+05	1.4225894+05	6.0463573+00	2.0300570+02	0.0000000+00	3.8546883+01	0.0000000+00
2.1600000+01	1.1936726+05	1.4083741+05	6.0463573+00	1.9206129+02	0.0000000+00	3.7038926+01	0.0000000+00
2.1600000+01	1.1936726+05	1.3944401+05	6.0463573+00	1.8115271+02	0.0000000+00	3.5479859+01	0.0000000+00
2.1600000+01	1.1936726+05	1.3807790+05	6.0463573+00	1.7027854+02	0.0000000+00	3.3868537+01	0.0000000+00
2.1600000+01	1.1936726+05	1.3673831+05	6.0463573+00	1.5943745+02	0.0000000+00	3.2203808+01	0.0000000+00
2.1600000+01	1.1936726+05	1.3542446+05	6.0463573+00	1.4862813+02	0.0000000+00	3.0484502+01	0.0000000+00
2.1600000+01	1.1936726+05	1.3413561+05	6.0463573+00	1.3784931+02	0.0000000+00	2.8709441+01	0.0000000+00
2.1600000+01	1.1936726+05	1.3287107+05	6.0463573+00	1.2709978+02	0.0000000+00	2.6877430+01	0.0000000+00
2.1600000+01	1.1936726+05	1.3163014+05	6.0463573+00	1.1637838+02	0.0000000+00	2.4987267+01	0.0000000+00
2.1600000+01	1.1936726+05	1.2993129+05	6.0463573+00	1.0141350+02	0.0000000+00	2.2241019+01	0.0000000+00
2.1600000+01	1.4370946+05	1.1936726+05	6.5321350+00	0.0000000+00	4.0904229+02	0.0000000+00	3.7530330+01
2.1600000+01	1.4225894+05	1.1936726+05	6.5032412+00	0.0000000+00	3.8687131+02	0.0000000+00	3.6162540+01
2.1600000+01	1.4083741+05	1.1936726+05	6.4749155+00	0.0000000+00	3.6491328+02	0.0000000+00	3.4747859+01
2.1600000+01	1.3944401+05	1.1936726+05	6.4471416+00	0.0000000+00	3.4316201+02	0.0000000+00	3.3285228+01
2.1600000+01	1.3807790+05	1.1936726+05	6.4199043+00	0.0000000+00	3.2161152+02	0.0000000+00	3.1773576+01
2.1600000+01	1.3673831+05	1.1936726+05	6.3931883+00	0.0000000+00	3.0025609+02	0.0000000+00	3.0211820+01
2.1600000+01	1.3542446+05	1.1936726+05	6.3669794+00	0.0000000+00	2.7909017+02	0.0000000+00	2.8598863+01
2.1600000+01	1.3413561+05	1.1936726+05	6.3412637+00	0.0000000+00	2.5810845+02	0.0000000+00	2.6933599+01
2.1600000+01	1.3287107+05	1.1936726+05	6.3160279+00	0.0000000+00	2.3730580+02	0.0000000+00	2.5214909+01
2.1600000+01	1.3163014+05	1.1936726+05	6.2912592+00	0.0000000+00	2.1667726+02	0.0000000+00	2.3441663+01
2.1600000+01	1.2993129+05	1.1936726+05	6.2573435+00	0.0000000+00	1.8808073+02	0.0000000+00	2.0865286+01

TT	KGL	KGT
6.2000000+01	4.8017234-01	8.7895420-01
6.9000000+01	4.8023393-01	8.7492766-01
6.6000000+01	4.7995916-01	8.7565291-01
7.0000000+01	4.7955836-01	8.7164170-01
8.0000000+01	4.9064181-01	8.6812695-01
8.0000000+01	4.8996043-01	8.6812695-01
8.0000000+01	4.8929830-01	8.6812695-01
8.0000000+01	4.8865492-01	8.6812695-01
8.0000000+01	4.8802977-01	8.6812695-01
8.0000000+01	4.8742237-01	8.6812695-01
8.0000000+01	4.8683224-01	8.6812695-01
8.0000000+01	4.8625895-01	8.6812695-01
8.0000000+01	4.8570204-01	8.6812695-01
8.0000000+01	4.8516111-01	8.6812695-01
8.0000000+01	4.8442985-01	8.6812695-01
-2.0000000+01	4.8015699-01	9.3787419-01
-1.5000000+01	4.8015699-01	9.3372566-01
-1.0000000+01	4.8015699-01	9.2965870-01
-5.0000000+00	4.8015699-01	9.2567097-01
0.0000000+00	4.8015699-01	9.2176028-01
5.0000000+00	4.8015699-01	9.1792444-01
1.0000000+01	4.8015699-01	9.1416140-01

QCT	QR1	QR2
618766+01	0.0000000+00	8.4612173+00
066838+01	0.0000000+00	5.0554572+00
431502+01	0.0000000+00	7.3425307+00
221813+01	0.0000000+00	6.8457387+00
000000+00	4.0004857+01	0.0000000+00
000000+00	3.8546883+01	0.0000000+00
000000+00	3.7038926+01	0.0000000+00
000000+00	3.5479859+01	0.0000000+00
000000+00	3.3868537+01	0.0000000+00
000000+00	3.2203808+01	0.0000000+00
000000+00	3.0484502+01	0.0000000+00
000000+00	2.8709441+01	0.0000000+00
000000+00	2.6877430+01	0.0000000+00
000000+00	2.4987267+01	0.0000000+00
000000+00	2.2241019+01	0.0000000+00
904229+02	0.0000000+00	3.7530330+01
687131+02	0.0000000+00	3.6162540+01
491328+02	0.0000000+00	3.4747859+01
316201+02	0.0000000+00	3.3285228+01
161152+02	0.0000000+00	3.1773576+01
025609+02	0.0000000+00	3.0211820+01
909017+02	0.0000000+00	2.8598863+01
810845+02	0.0000000+00	2.6933599+01
730580+02	0.0000000+00	2.5214909+01
667726+02	0.0000000+00	2.3441663+01
808073+02	0.0000000+00	2.0865286+01

1.5000000+01	4.8015699-01	9.1046918-01
2.0000000+01	4.8015699-01	9.0684586-01
2.5000000+01	4.8015699-01	9.0328960-01
3.2000000+01	4.8015699-01	8.9842005-01

TYPE #END# STATEMENT EXECUTED.
CARDS REMAINING IN DECK ARE--

MAY 20 66 21 21.4

References

1. Andres, Ronald P., " Homogeneous Nucleation from the Gas Phase", Ind. Eng. Chem., 57, No. 10, 9 (1965)

2. Barrow, R.F., and L.S. Han, " Heat and Mass Transfer to a Cryosurface in Free Convection", J. Heat Transfer, A.S. M.E. Series C, 87, No. 4 (1965)

3. Bird, R.B., Stewart, W.E., and E.N. Lightfoot, Transport Phenomena, John Wiley and Sons, Inc., New York, N.Y. (1960)

4. Brailsford, A.D., and K.G. Major, " Thermal Conductivity of Aggregates of Several Phases Including Porous Materials", Brit. J. Applied Physics, 15, No.3, 313 (March 1964)

5. Bueckner, H., and G. Harvay, " Heat Transfer Coefficient of Inviscid Fluid Freezing onto Moving Heat Sink", Trans. A.S.M.E., J. Heat Transfer, 85, No. 3, 246(Aug.1963)

6. Canterbury, Jack, and Ellis M. Killgare, " The Investigation of Heat Transfer and Frost Formation Across a Plane Surface Held at Sub-freezing Temperatures", National Science Found. Report, NSF - GP - 552, Mech. Eng. Dept., Louisiana Poly. Inst. (1965)

7. Chen, M.M., and W. Rohsenow, " Heat and Momentum Transfer Inside Frosted Tubes - Experiment and Theory ", J. Heat Transfer, C 86, No. 3, 334 (1964)

8. Chung, P. M., and A.B. Algren, " Frost Formation and Heat Transfer on a Cylindrical Surface in Humid Air Cross Flow", Part I Exp. Study, Heating, Piping and Air Conditioning Journal, 171 (Sep. 1958)

9. Chung, P.M., and A. B. Algren, " Frost Formation and Heat Transfer on a Cylindrical Surface in Humid Air Cross Flow", Part II, Theoretical Study , Heating, Piping and Air Conditioning Journal, 115 (Oct. 1958)

10. Coles, W., and R. Ruggeri, " Experimental Investigation of the Sublimation of Ice at Subsonic and Supersonic Speeds and its Relation to Heat Transfer ", N.A.C.A. Tech. Note No. 3104, (March 1954)

11. Coles, W.D., " Experimental Investigation of Thermal Conductivity of Low Density Ice", N.A.C.A. Tech. Note No. 3143, (1954)

12. Corsin, Stanley, " Extended Applications of the Hot-Wire Anemometer ", N.A.C.A. Tech. Note No. 1864 (April 1949)

13. Dibbern, D., " The Formation of Frost and Snow During the Cooling Process of Vapor-Gas Mixtures in Counterflow Heat Exchangers ", Kältetechnick, 16, No. 6, 167(1964)

14. Everett, D.H., and F.S. Stone , The Structure and Properties of Porous Materials ", Academic Press, Butterworths, London (1958)

15. Gomelauri, " Influence of Two-Dimensional Artificial Roughness on Convective Heat Transfer ", Int. J. of Heat and Mass Transfer, 7, 653(1964)

16. Gretz, R.D., and G.M. Pound, " Vapor -Solid Nucleation", Technical Report Submitted to the National Science Foundation, N.S.F. Grant G 21538, Metals Research Lab., Carnegie Institute of Tech.,(june 1963)

17. Gretz, R.D. " Epitaxi and Oriented Overgrowth of Vapor Deposited Materials ", Six Quarterly Literature Review, Battele Memorial Institute, Columbus, Ohio(Oct.1963)

18. Hausen, H., " Freezing Out of Vapors from Gas-Vapor Mixtures", Problems of Low Temperature Physics and Thermodynamics, Symposium Publications, Pergamon Press, New York, (1962)

19. Hsu, S.T., Engineering Heat Transfer , D. Van Nostrand Company, Inc., New Jersey (1963)

20. Kingery, W.D. (editor), Ice and Snow, Properties, Proces ses, and Applications, Proceedings of a Conference Held at the Mass. Inst. of Tech.,Feb.12-16 (1962).The M.I.T. Press.

21. Koh, J.C.Y., and P.E. Grafton, " Skin Friction, Heat Transfer and Condensation Rate for Binary Cryogenic Flow Over a Flat Plate ", Advances in Cryogenic Engineering, 7,367(1961)

22. Kondrat'eva, A.S., " Thermal Conductivity of Snow Cover and Physical Processes Caused by the Temperature Gradient", U.S. Army , Corps of Engineers, Snow Ice, and Premafrost Research Establishment, S.I.P.R.E. Translation No.22(1954)

23. Libby, P.A., and Shun Chen, " The Growth of a Deposited Layer on a Cold Surface ", Int. J. Heat and Mass Transfer, 8, 395 (1965)

24. Loper, J.L., " Frost Formation Upon a Thin Aluminum Tank Containing Liquid Oxigen ",Transactions A.S.HR.A.E.,66, 104 (1960)

25. Nakaya, Ukichiro, Snow Crystals, Natural and Artificial, Harvard University Press, Cambridge, Mass. (1954)

26. Richards, R.J., D.K. Edmonds , and R.B. Jacobs, " Heat Transfer Between a Cryo-Surface and a Controlled Atmosphere ", Experimental Investigation, Cryogenic Eng. Lab., National Bureau of Standards, Boulder, Colorado, International Institute of Refrigeration, 89 (Aug.1962)

27. Rische, E.A., " Freezing -Out of Gas-Vapor Mixtures in Forced Tubular Flow ", Chemie Ingenieur Technik, 29,603 (1957)

28. Schlichting, Hermann, Boundary Layer Theory, 4th Ed., McGraw Hill Series in Mechanical Engineering, New York, (1960)

29. Shedden, J.A., " A Study of Mass Transfer Rates Through Boundary Layers Subjected to Accelerated Flows or Varying Turbulence Intensity ", Ph.D. Thesis, Lehigh University, Chemical Engineering Dept., (1965)

30. Sibbit, W.L., W.E. Fontaine, and J.P, Dotson, " Ice Formation on Metal Surfaces ", Refrigerating Engineering, 62, (1954)

31. Smith, R.V., E.K. Edmonds, E.G.F. Brentari, and R.J. Richards, " Analysis of Frost Formation on a Cryo-surface", Advances in Cryogenic Engineering, 9,88 (1963)

32. Sparrow, E.M., and S.H. Liu, " Condensation Heat Transfer in the Presence of a Non-Condensable Gas ", J. Heat Transfer, C 86, No. 3, 430 (1964)

33. Stewart, Johnson, and Olien, " Second Progress Report on Cryogenic Data Center Activities for the Period Ending June 30, 1965 ", N.B.S. Cryog. Division Reports.

34. Stoecker, W.F., " Frost Formation on Refrigerating Coils ", A.S.H.R.A.E. Transactions, 66, 91 (1960)

35. Sugawara, A., and Y. Yoshizawa, " An Investigation of the Conductivity of Porous Materials and its Application to Porous Rock ", Australian Journal of Physics,14 , 469 (1961)

36. Thermo Systems Inc., " Application of the Heat Flux System in Low Temperature Gases and Liquids ", Technical Bulleting No.4, Thermo-Systems Inc., Minneapolis Minnesota.

37. Van Gundy, D.A., and J.R, Uglum, " Heat Transfer to an Uninsulated Surface at 20°K ", Advances in Cryogenic Engineering, 7, 377 (1961)

38. Weber, Martin E., " Heat Transfer to a Cryogenic Surface Under Frosting Conditions ", Ph.D. Thesis, Dept. of Chem. Eng. , Mass. Inst. of Tech. , April(1964)

39. Whitehurst, Charles A., " An Investigation of Heat and Mass Transfer by Free Convection from Humid Air to a Metal Plate Under Frosting Conditions ", Ph.D. Dissertation, Mechanical Engineering Department, Agricultural and Mechanical College of Texas, (Jan. 1962)

40. Whitehurst, C.H., " Heat and Mass Transfer to a Metal Plate ", A.S.H.R.A.E. Journal , 4, (1962)

41. Woodside,W., " Calculation of the Thermal Conductivity of Porous Media ", Can. J. Physics, 36, 815 (1958)

42. Yozida, Z., et al, " Physical Studies on Deposited Snow and Thermal Properties", Contributions from the Institute of Low Temperature Science, No. 7, 19, Hokkaido University, Sappow, Japan (1955)

Vita

Name: Gabriel Biguria O.

Place of Birth: Guatemala City, Guatemala

Date of Birth: August 1, 1941

Parents: Gabriel Biguria S. and Concha O. de Biguria

Education: Elementary school and high school at the American School in Guatemala City; Chauncy Hall School, Boston, Massachusetts; Case Institute of Technology, Cleveland, Ohio

Degrees: B.S. in Chemical Engineering, Case , 1963

Profesional and Honorary Societies: AX² Honorary Society for Chemists and Chemical Engineers, The American Institute for Chemical Engineers, and the American Chemical Society

Professional Experience:

Research Assistant, International Nickel Co., Research Laboratories, Bayonne, N.J., Summer 1962